Virtual and real experiments

synergetic interplay

L. Udby

University of Copenhagen, Niels Bohr Institute, Denmark

INSIS 2012

Outline

- What is a virtual (neutron) experiment?
- What can it be used for?

1. EXAMPLE 1: PEAK BROADENING IN LSCO+O
2. EXAMPLE 2: PHASESHIFT BY REFRACTING PRISM IN SESANS

Outline

- What is a virtual (neutron) experiment?
- What can it be used for?
  1. EXAMPLE 1: PEAK BROADENING IN LSCO+O
  2. EXAMPLE 2: PHASESHIFT BY REFRACTING PRISM IN SESANS

What is a virtual (neutron) experiment?

- The neutrons rays must have absolute intensity units and should be traced through the whole instrument, from source to detector.
- The description of the instrument should be as close as possible to the reality. This is in particular the case for the sample.
- The virtual instrument is controlled like the real instrument, and the resulting data are analyzed like real data.

More in Lefmann et al JNR **16**(3-4), 97-111 (2008)

What is a virtual (neutron) experiment?

- The neutrons rays must have absolute intensity units and should be traced through the whole instrument, from source to detector.
- The description of the instrument should be as close as possible to the reality. This is in particular the case for the sample.
- The virtual instrument is controlled like the real instrument, and the resulting data are analyzed like real data.

More in Lefmann et al JNR **16**(3-4), 97-111 (2008)

What is a virtual (neutron) experiment?

- The neutrons rays must have absolute intensity units and should be traced through the whole instrument, from source to detector.
- The description of the instrument should be as close as possible to the reality. This is in particular the case for the sample.
- The virtual instrument is controlled like the real instrument, and the resulting data are analyzed like real data.

More in Lefmann et al JNR **16**(3-4), 97-111 (2008)

What is a virtual (neutron) experiment?

- The neutrons rays must have absolute intensity units and should be traced through the whole instrument, from source to detector.
- The description of the instrument should be as close as possible to the reality. This is in particular the case for the sample.
- The virtual instrument is controlled like the real instrument, and the resulting data are analyzed like real data.

More in Lefmann et al JNR **16**(3-4), 97-111 (2008)

What can virtual experiment be used for?

- Instrument upgrade and design
- Teaching and learning NS
- Separation of scattering contributions from sample and sample environment.
- Analysis of real experimental data

1. Peak broadening of superstructures of the HTSC $\mathrm{Lab}_{\mathrm{Sr}}\mathrm{CuO}_{\mathrm{Sr}}$ measured at RESAF-TAS @ PSI
2. Refracting prism measured at the SESANS @ Delft

What can virtual experiment be used for?

- Instrument upgrade and design

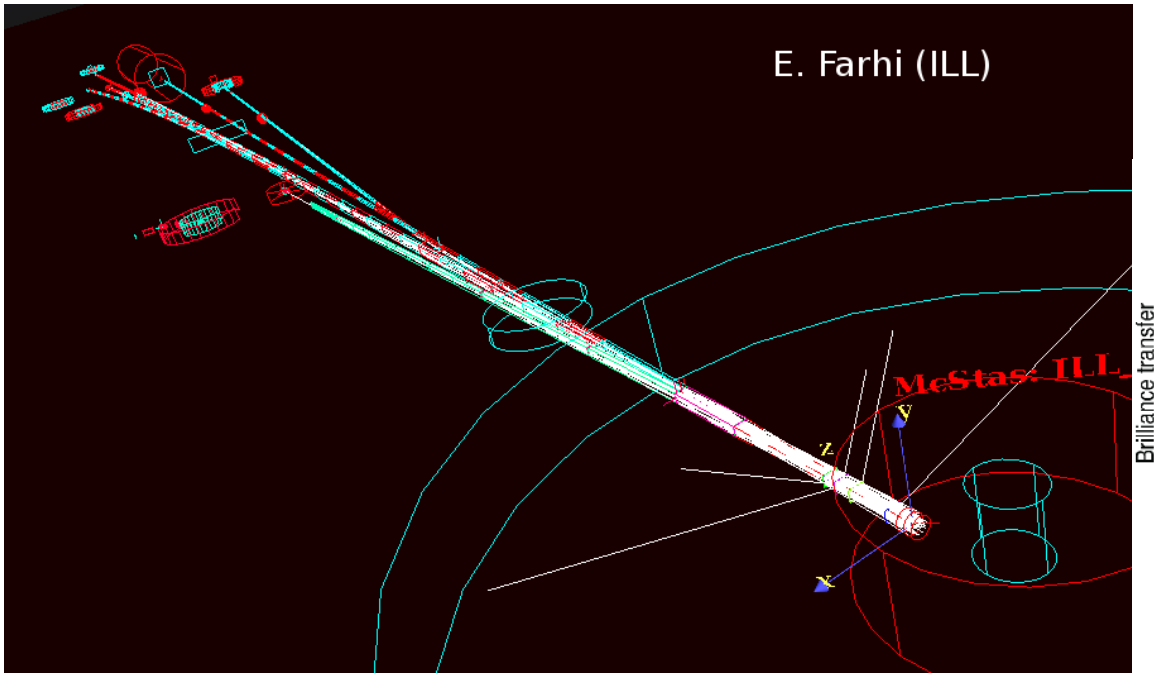

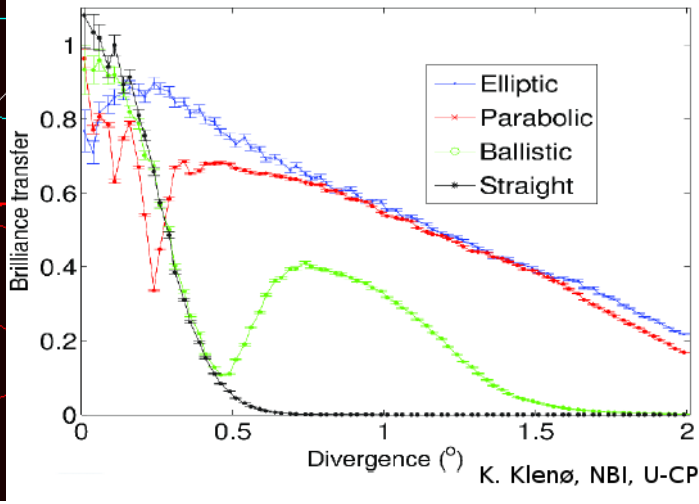

- Teaching and learning NS
- Separation of scattering contributions from sample and sample environment.
- Analysis of real experimental data
  1. Peak broadening of superstructures of the HTSC $La_{2-x}Sr_xCuO_{4+y}$ measured at RITA-II TAS @ PSI.

What can virtual experiment be used for?

- Instrument upgrade and design
- Teaching and learning NS
- Separation of scattering contributions from sample and sample environment.
- Analysis of real experimental data
  1. Peak broadening of superstructures of the HTSC $La_{2-x}Sr_xCuO_{4+y}$ measured at RITA-II TAS @ PSI.
  2. Refracting prism measured at the SESANS @ Delft

What can virtual experiment be used for?

- Instrument upgrade and design
- Teaching and learning NS

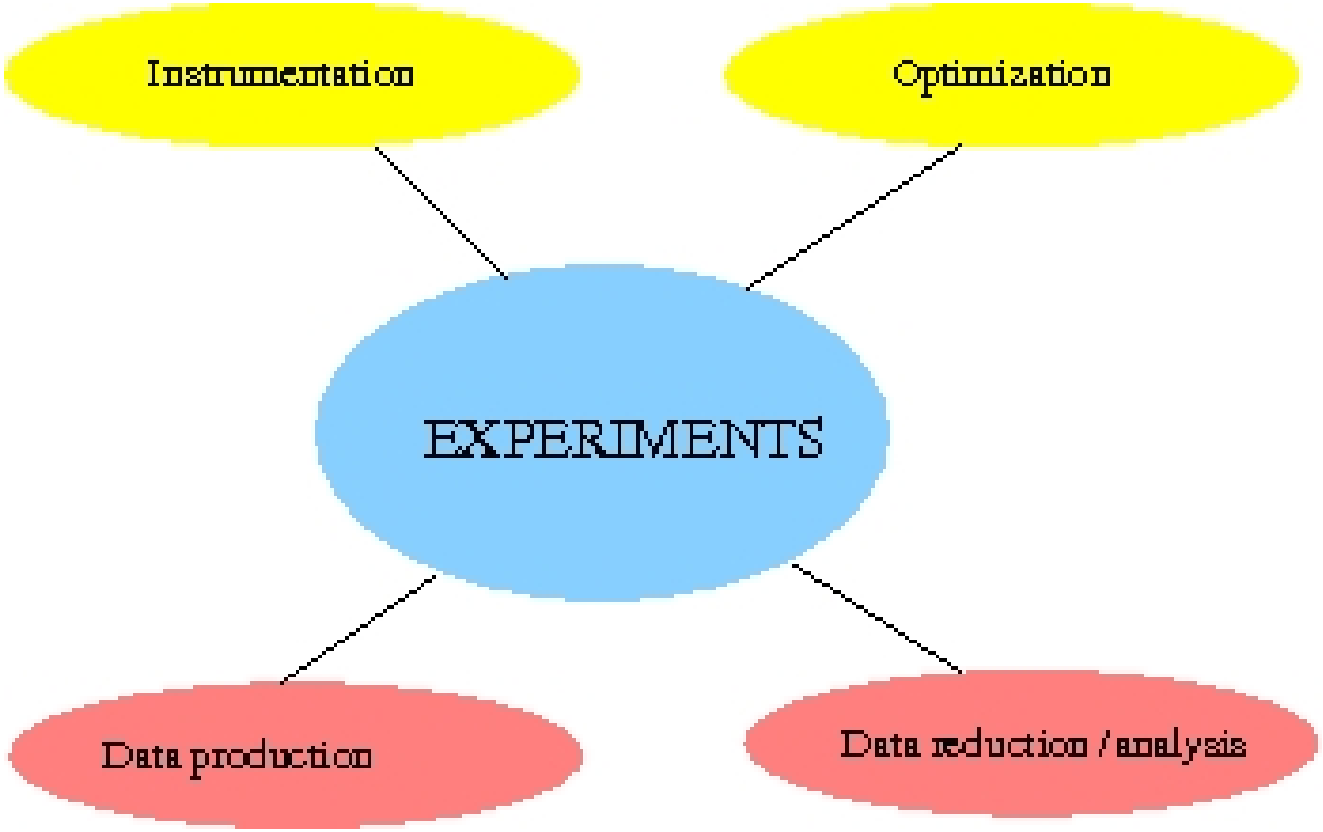

- Separation of scattering contributions from sample and sample environment.
- Analysis of real experimental data

What can virtual experiment be used for?

- Instrument upgrade and design
- Teaching and learning NS

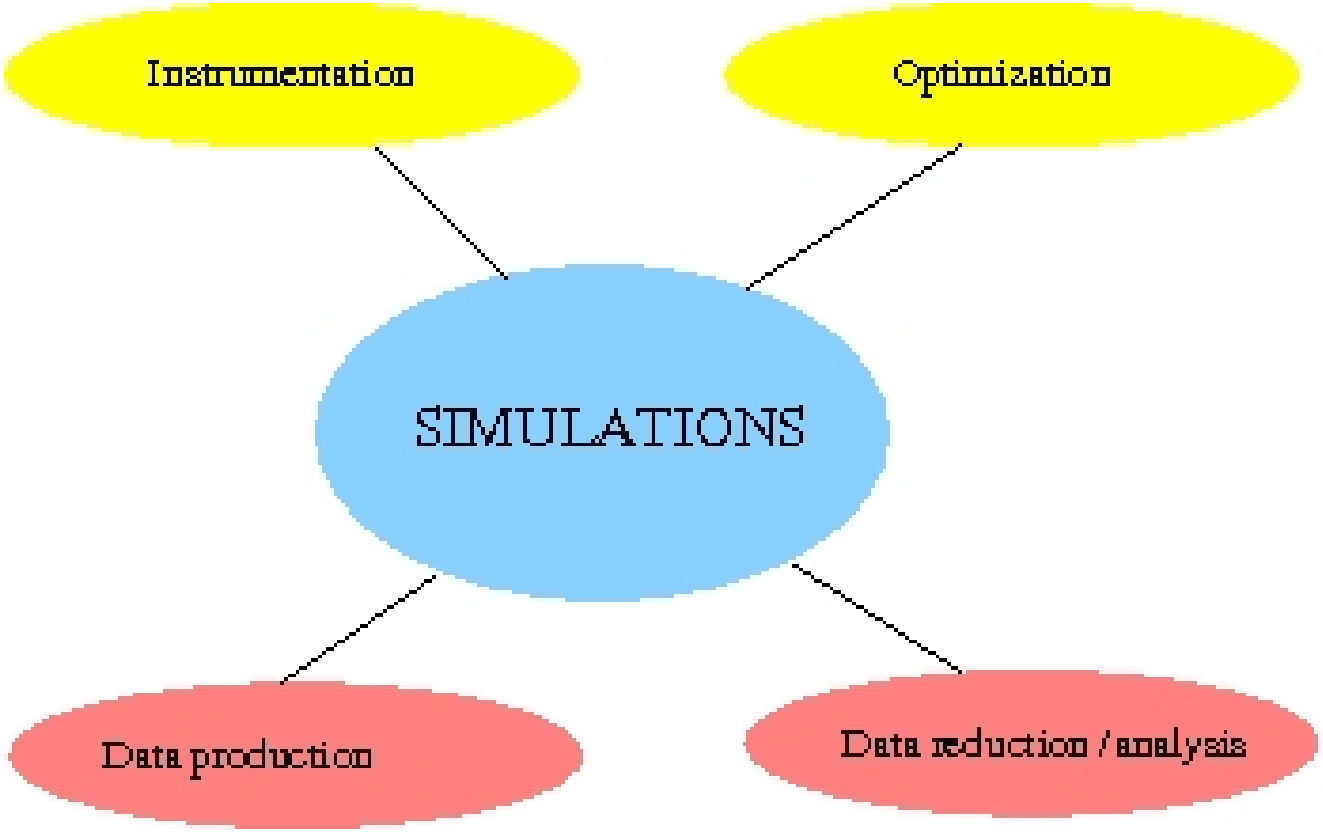

- Separation of scattering contributions from sample and sample environment.
- Analysis of real experimental data

What can virtual experiment be used for?

- Instrument upgrade and design
- Teaching and learning NS
  NMI3 E-LEARNING PORTAL COMING SOON!
- Separation of scattering contributions from sample and sample environment.
- Analysis of real experimental data
  1. Peak broadening of superstructures of the HTSC $La_{2-x}Sr_xCuO_{4+y}$ measured at RITA-II TAS @ PSI.
  2. Refracting prism measured at the SESANS @ Delft

What can virtual experiment be used for?

- Instrument upgrade and design
- Teaching and learning NS
- Separation of scattering contributions from sample and sample environment. Example TOF on liquid Ge

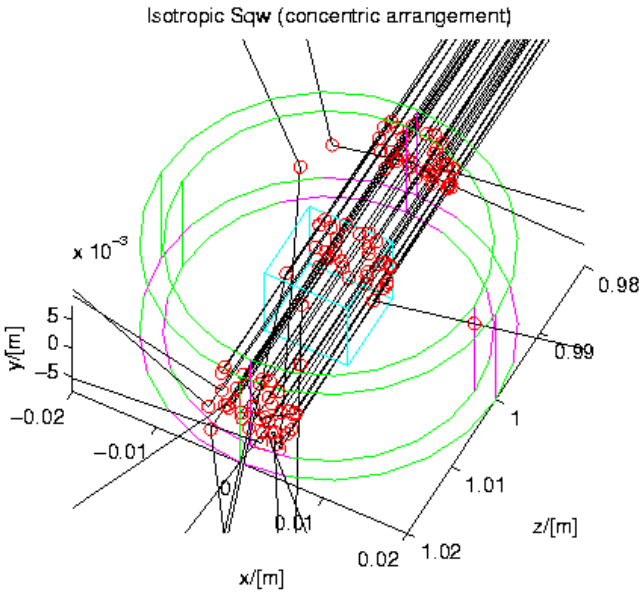

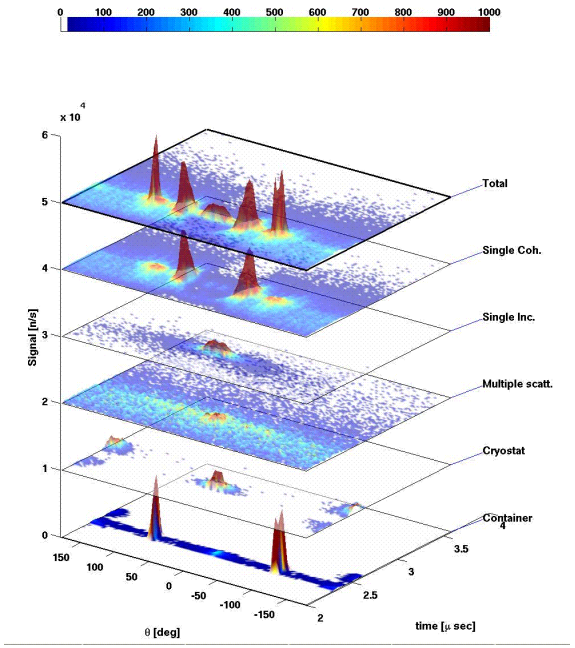

E. Farhi, M. Johnson, V. Hugouvieux and W. Kob, ILL Annual Report (2006) 87

- Analysis of real experimental data

What can virtual experiment be used for?

- Instrument upgrade and design
- Teaching and learning NS
- Separation of scattering contributions from sample and sample environment.
- Analysis of real experimental data

1. Peak broadening of superstructures of the HTSC $La_{2-x}Sr_xCuO_{4+y}$ measured at RITA-II TAS @ PSI.
2. Refracting prism measured at the SESANS @ Delft

What can virtual experiment be used for?

- Instrument upgrade and design
- Teaching and learning NS
- Separation of scattering contributions from sample and sample environment.
- Analysis of real experimental data
  Two examples (rest of the talk):
  1. Peak broadening of superstructures of the HTSC $La_{2-x}Sr_xCuO_{4+y}$ measured at RITA-II TAS @ PSI.
  2. Refracting prism measured at the SESANS @ Delft

What can virtual experiment be used for?

- Instrument upgrade and design
- Teaching and learning NS
- Separation of scattering contributions from sample and sample environment.
- Analysis of real experimental data
  1. Peak broadening of superstructures of the HTSC $La_{2-x}Sr_xCuO_{4+y}$ measured at RITA-II TAS @ PSI.
  2. Refracting prism measured at the SESANS @ Delft

EXAMPLE 1 - Virtual experiment Outline

Single-crystal sample

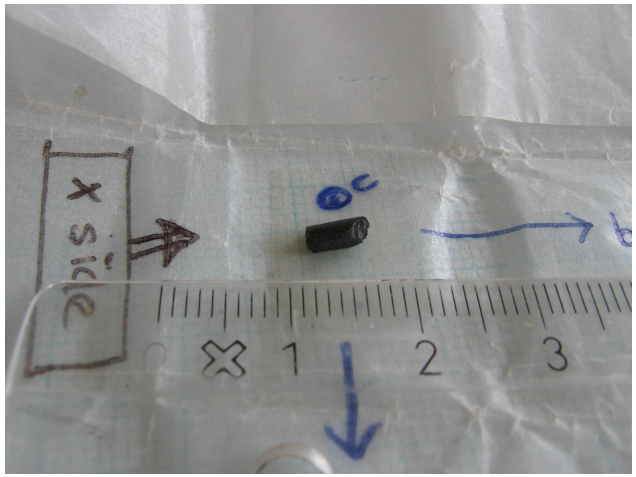

Finite size peak broadening?

McStas VE HOW–TO

INSTRUMENT

- Build instrument including all collimators
- Test instrument on powder 2θ scan
- Test instrument energy resolution on Vanadium

SINGLE CRYSTAL

- Set samplesize
- Set sample mosaicity vs. rocking curve
- Set uncertainty in lattice parameter vs longitudinal scan

MORPHOLOGY

- Perform VE corresponding to instrumental resolution limited experimental data
- Deconvolute finite size peak broadening from experimental data by comparing to VE data

McStas

V-RITA-II

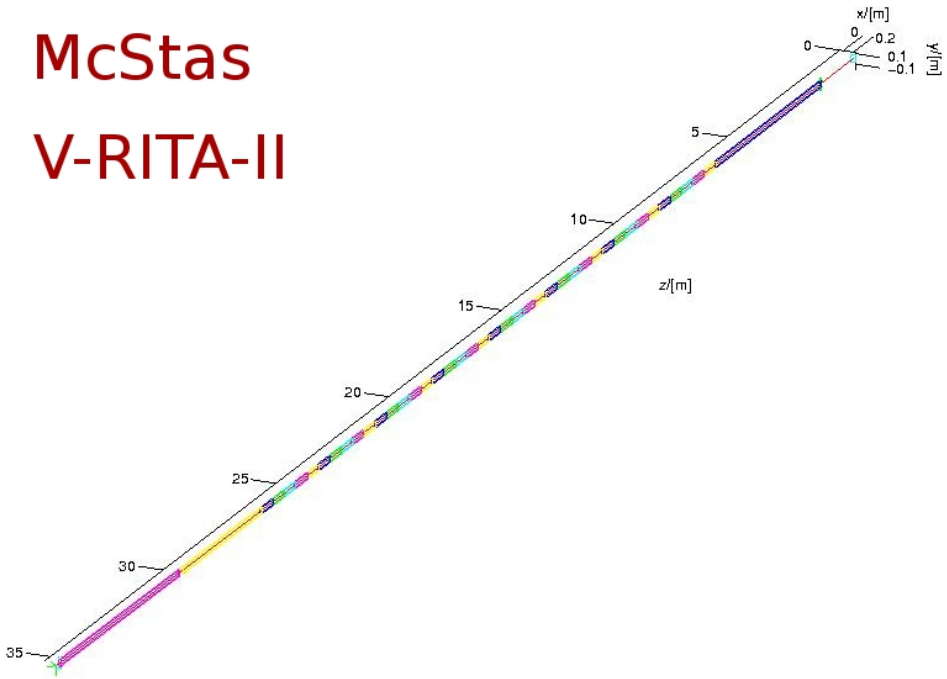

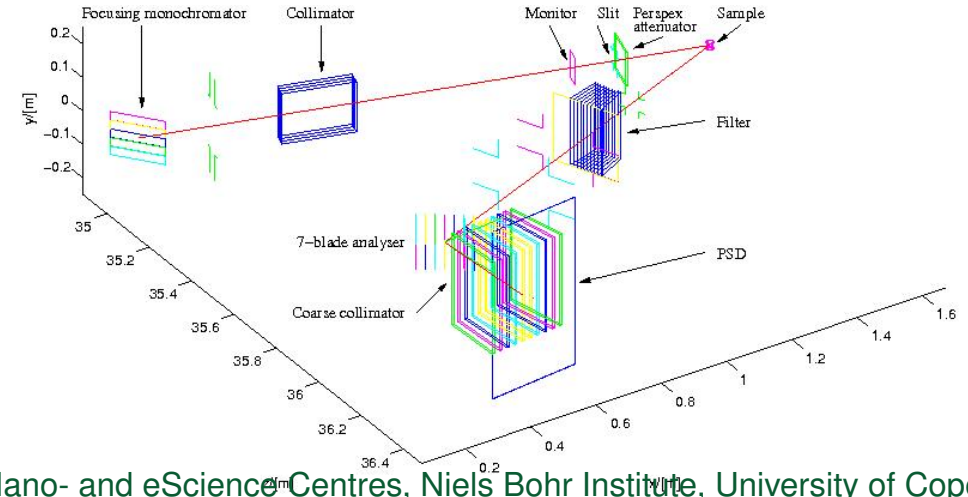

RITA-II TAS @ PSI with vertically focusing monochromator and multiblade analyser. Effective instrumental resolution and thereby the linewidth of a particular scan depends on

- Divergence of the beam before the monochromator: Size of source, geometry and m-values of guide elements
- Mosaicity of the monochromator
- Mosaicity of the analyser
- Geometrical factors: Sizes of components and distances between them
- Divergence of collimators
- Point-spread function of the position sensitive detector (PSD)
- Absolute energy of the incoming and scattered beam
- Sample parameters
  - shape/size (all samples including incoherent scatterer, powder, single-crystal)
  - particle size in sample (powder)
  - mosaicity and uncertainty in lattice parameters (single-crystal)

McStas

V-RITA-II

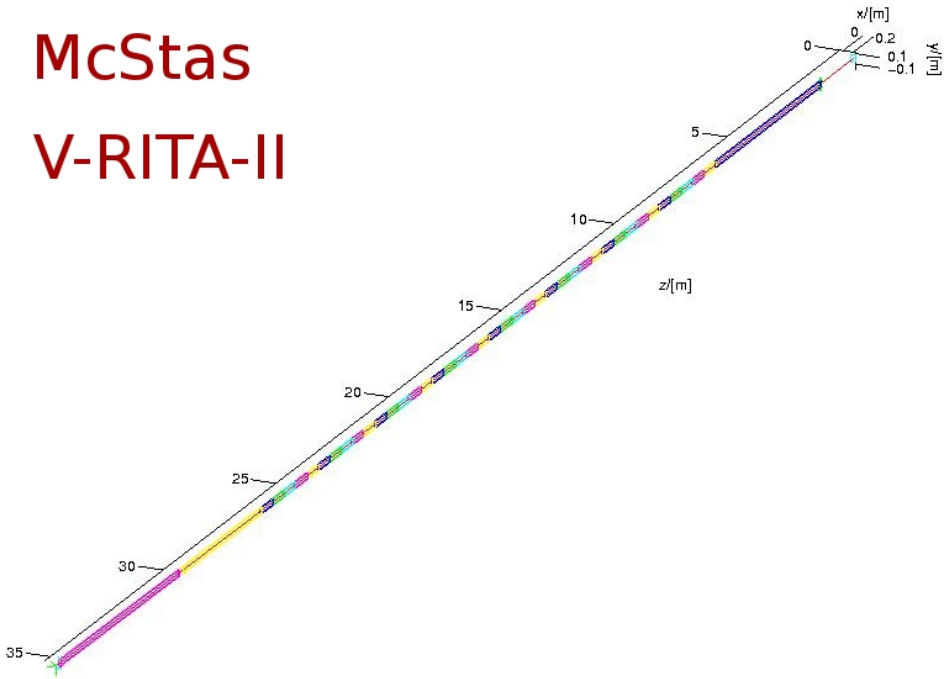

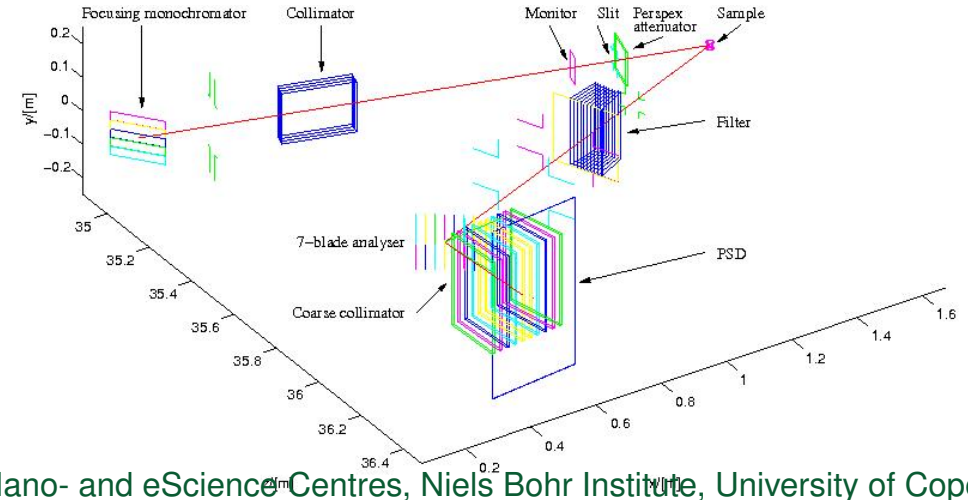

RITA-II TAS @ PSI with vertically focusing monochromator and multiblade analyser. Effective instrumental resolution and thereby the linewidth of a particular scan depends on

- Divergence of the beam before the monochromator: Size of source, geometry and m-values of guide elements
- Mosaicity of the monochromator
- Mosaicity of the analyser
- Geometrical factors: Sizes of components and distances between them
- Divergence of collimators
- Point-spread function of the position sensitive detector (PSD)
- Absolute energy of the incoming and scattered beam
- Sample parameters
  - shape/size (all samples including incoherent scatterer, powder, single-crystal)
  - particle size in sample (powder)
  - mosaicity and uncertainty in lattice parameters (single-crystal)

McStas

V-RITA-II

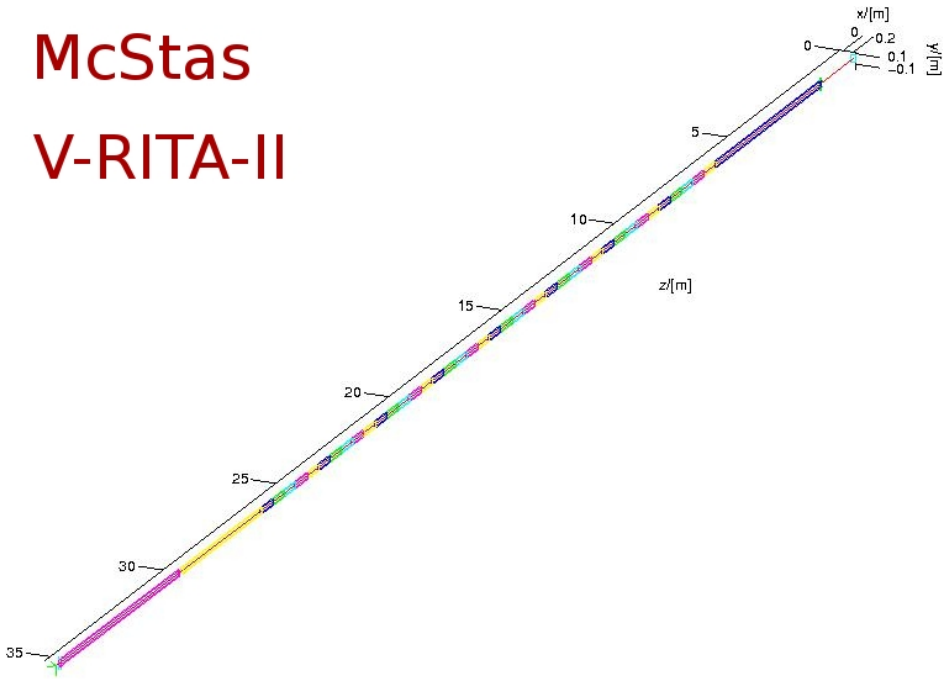

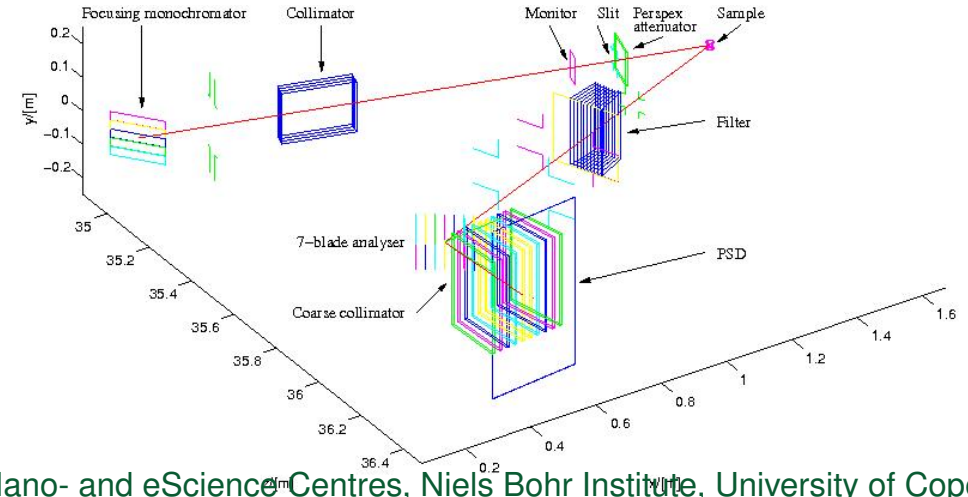

RITA-II TAS @ PSI with vertically focusing monochromator and multiblade analyser. Effective instrumental resolution and thereby the linewidth of a particular scan depends on

- Divergence of the beam before the monochromator: Size of source, geometry and m-values of guide elements
- Mosaicity of the monochromator
- Mosaicity of the analyser
- Geometrical factors: Sizes of components and distances between them
- Divergence of collimators
- Point-spread function of the position sensitive detector (PSD)
- Absolute energy of the incoming and scattered beam
- Sample parameters
  - shape/size (all samples including incoherent scatterer, powder, single-crystal)
  - particle size in sample (powder)
  - mosaicity and uncertainty in lattice parameters (single-crystal)

McStas

V-RITA-II

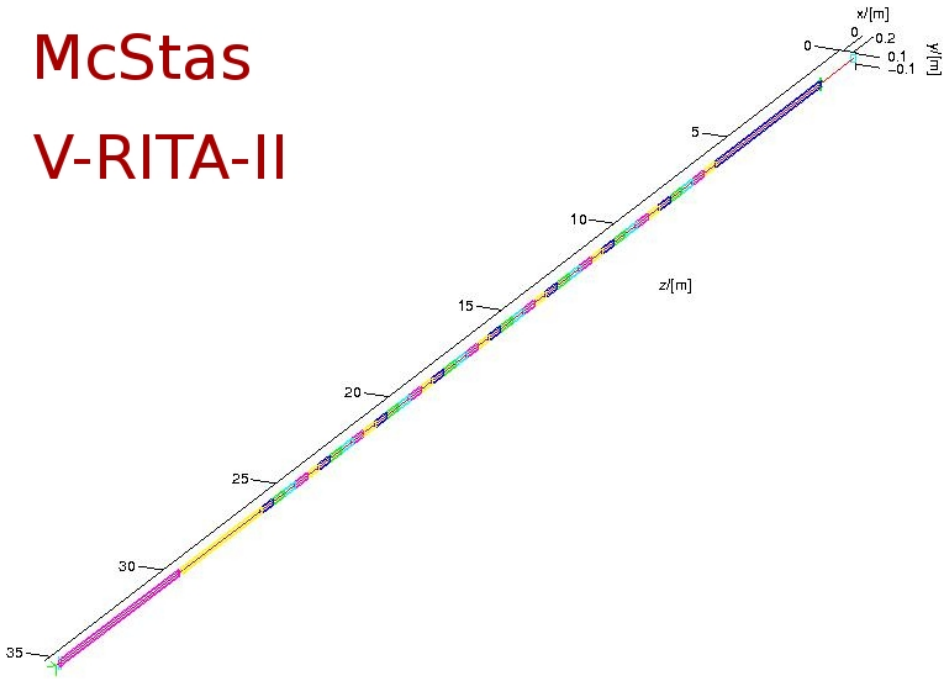

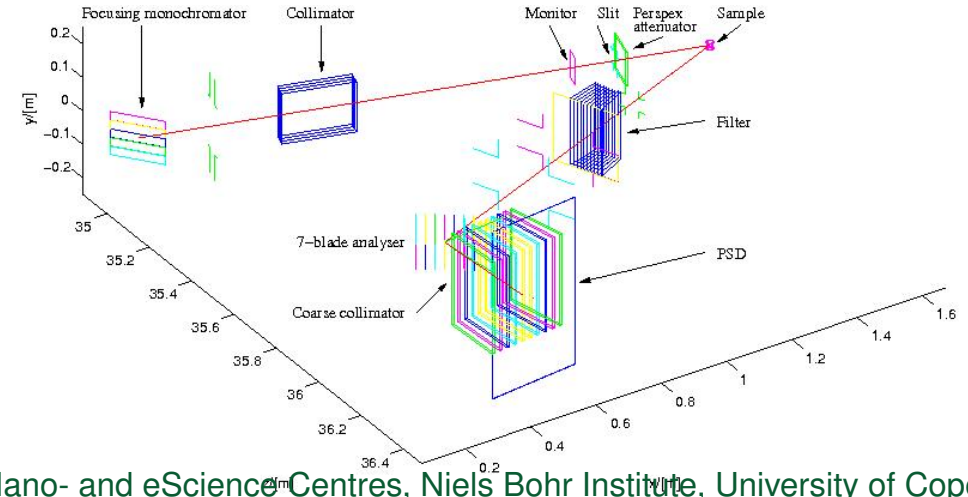

RITA-II TAS @ PSI with vertically focusing monochromator and multiblade analyser. Effective instrumental resolution and thereby the linewidth of a particular scan depends on

- Divergence of the beam before the monochromator: Size of source, geometry and m-values of guide elements
- Mosaicity of the monochromator
- Mosaicity of the analyser
- Geometrical factors: Sizes of components and distances between them
- Divergence of collimators
- Point-spread function of the position sensitive detector (PSD)
- Absolute energy of the incoming and scattered beam
- Sample parameters
  - shape/size (all samples including incoherent scatterer, powder, single-crystal)
  - particle size in sample (powder)
  - mosaicity and uncertainty in lattice parameters (single-crystal)

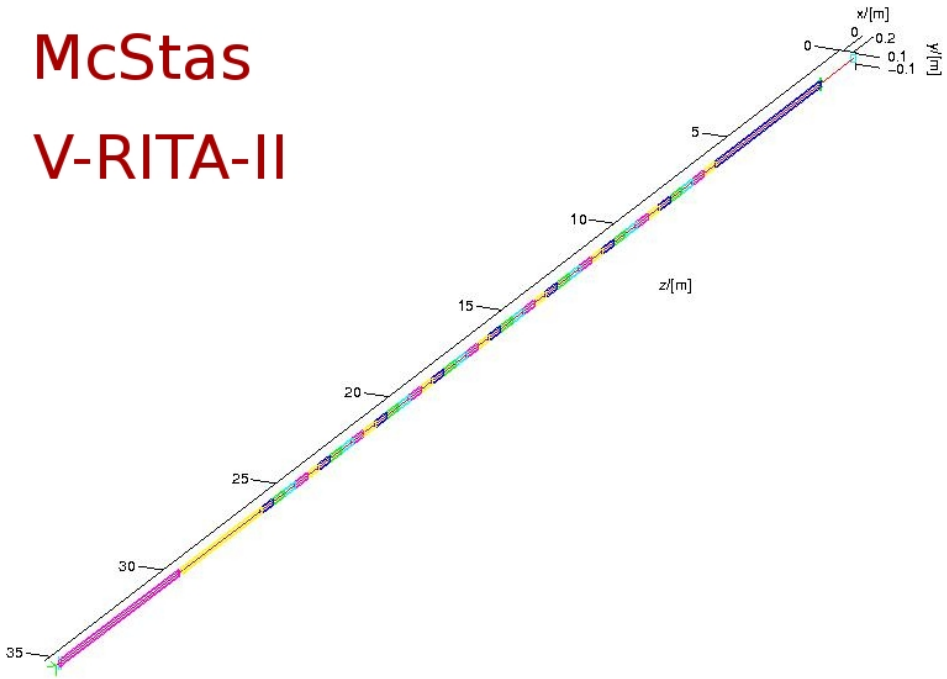

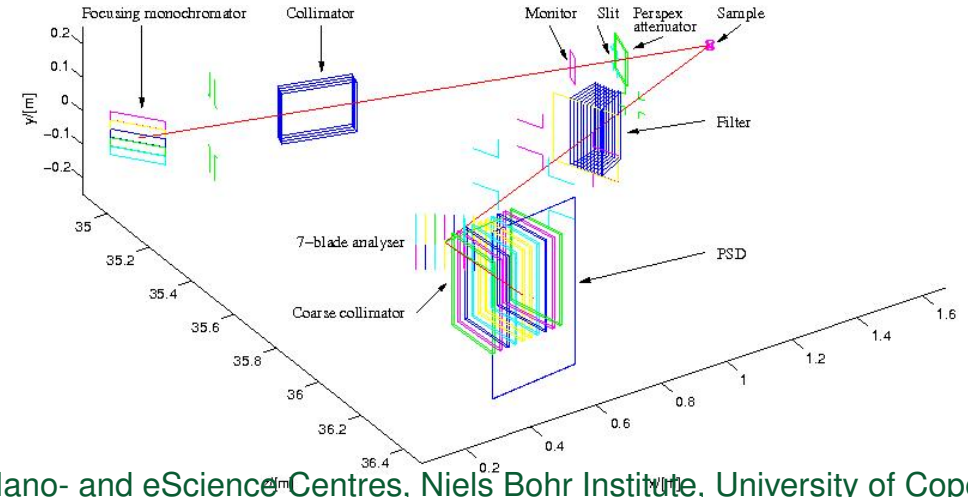

RITA-II TAS @ PSI with vertically focusing monochromator and multiblade analyser. Effective instrumental resolution and thereby the linewidth of a particular scan depends on

- Divergence of the beam before the monochromator: Size of source, geometry and m-values of guide elements
- Mosaicity of the monochromator
- Mosaicity of the analyser
- Geometrical factors: Sizes of components and distances between them
- Divergence of collimators
- Point-spread function of the position sensitive detector (PSD)
- Absolute energy of the incoming and scattered beam
- Sample parameters
  - shape/size (all samples including incoherent scatterer, powder, single-crystal)
  - particle size in sample (powder)
  - mosaicity and uncertainty in lattice parameters (single-crystal)

McStas

V-RITA-II

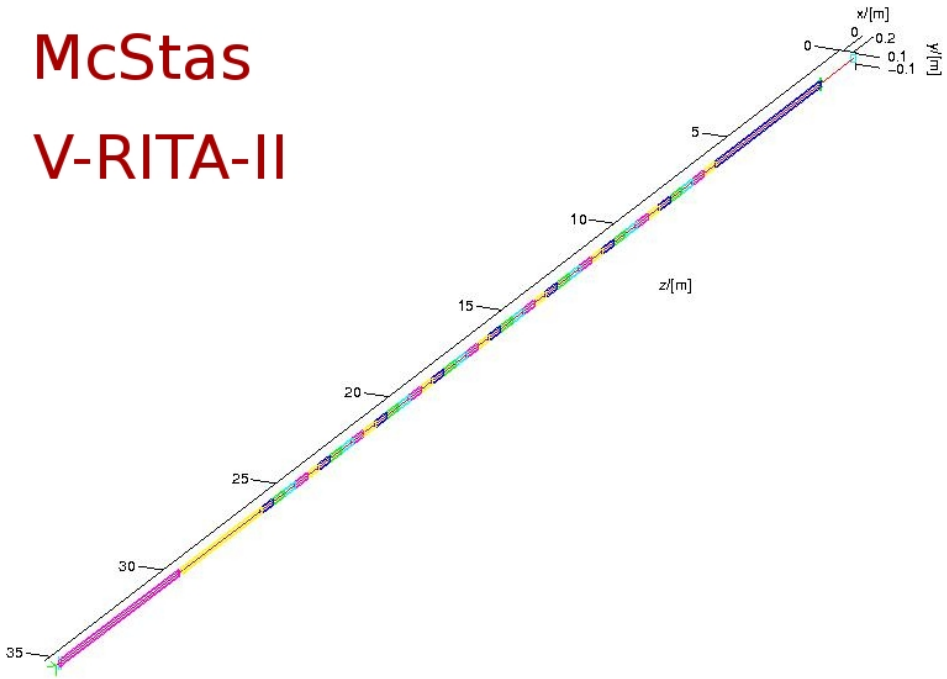

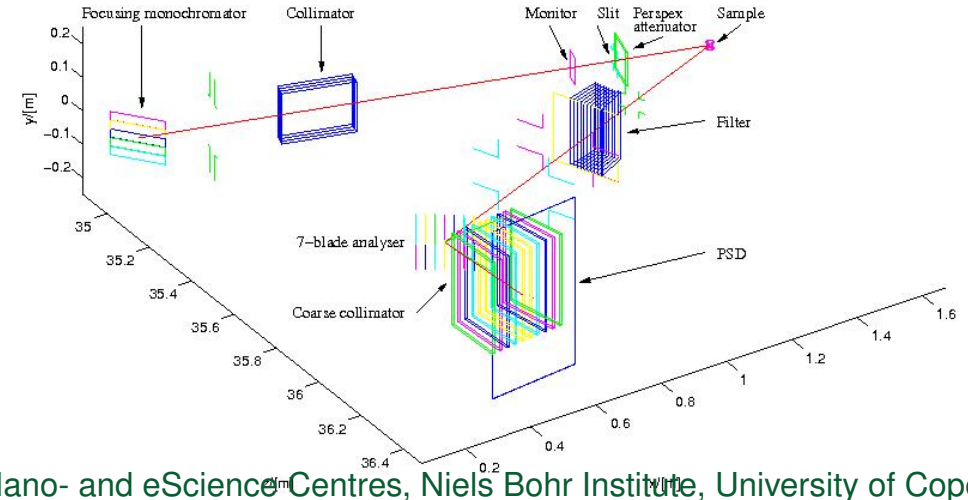

RITA-II TAS @ PSI with vertically focusing monochromator and multiblade analyser. Effective instrumental resolution and thereby the linewidth of a particular scan depends on

- Divergence of the beam before the monochromator: Size of source, geometry and m-values of guide elements
- Mosaicity of the monochromator
- Mosaicity of the analyser
- Geometrical factors: Sizes of components and distances between them
- Divergence of collimators
- Point-spread function of the position sensitive detector (PSD)
- Absolute energy of the incoming and scattered beam
- Sample parameters
  - shape/size (all samples including incoherent scatterer, powder, single-crystal)
  - particle size in sample (powder)
  - mosaicity and uncertainty in lattice parameters (single-crystal)

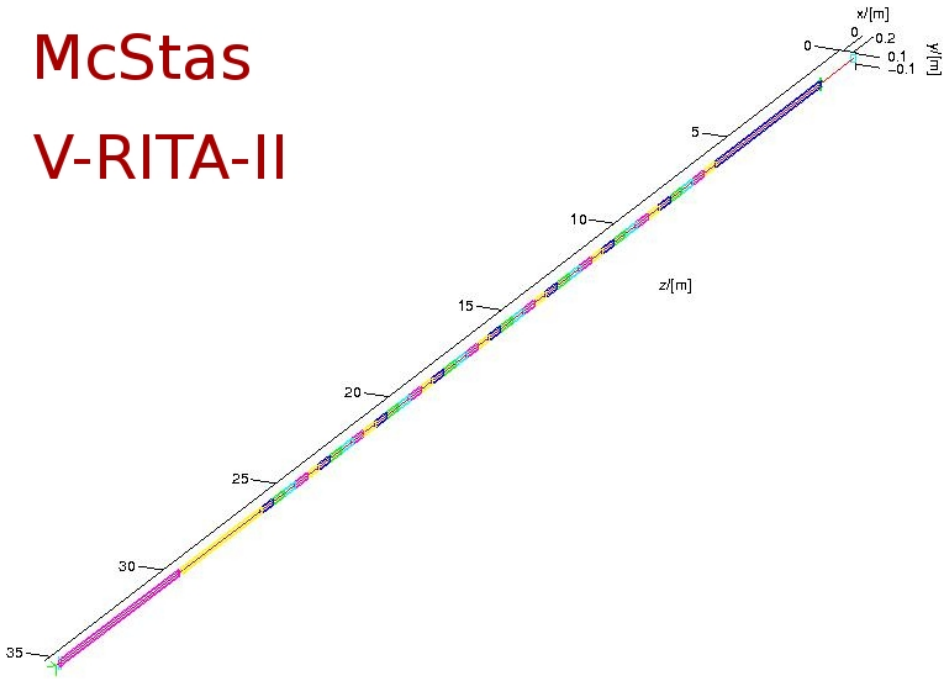

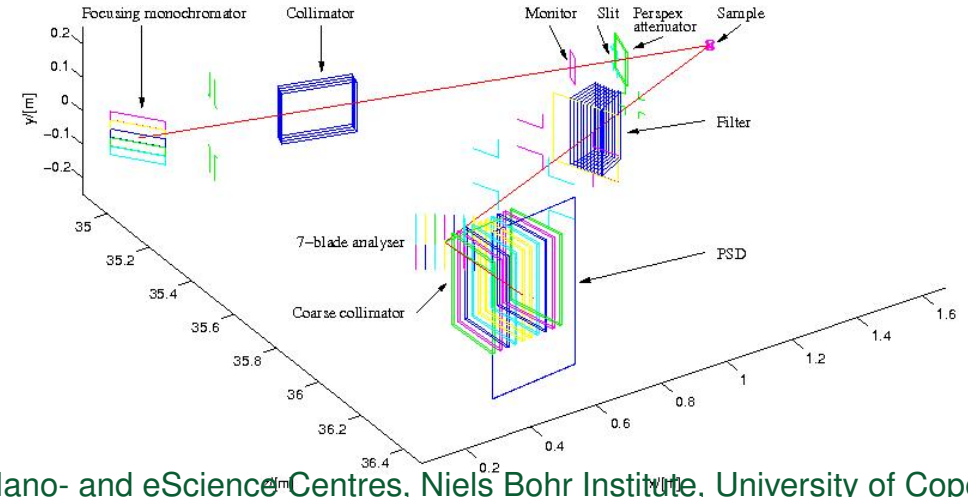

RITA-II TAS @ PSI with vertically focusing monochromator and multiblade analyser. Effective instrumental resolution and thereby the linewidth of a particular scan depends on

- Divergence of the beam before the monochromator: Size of source, geometry and m-values of guide elements
- Mosaicity of the monochromator
- Mosaicity of the analyser
- Geometrical factors: Sizes of components and distances between them
- Divergence of collimators
- Point-spread function of the position sensitive detector (PSD)
- Absolute energy of the incoming and scattered beam
- Sample parameters
  - shape/size (all samples including incoherent scatterer, powder, single-crystal)
  - particle size in sample (powder)
  - mosaicity and uncertainty in lattice parameters (single-crystal)

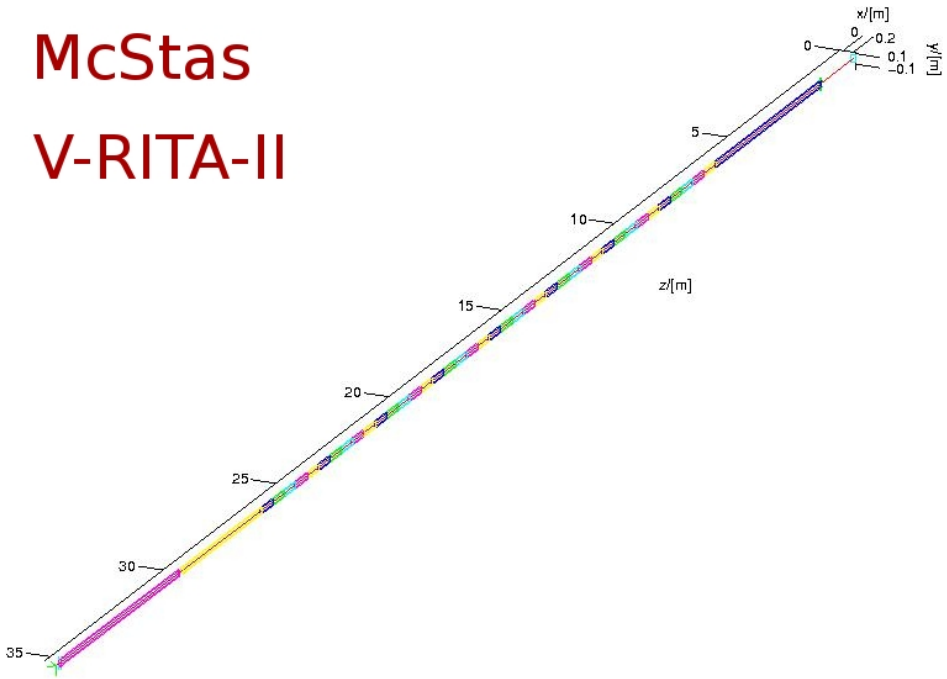

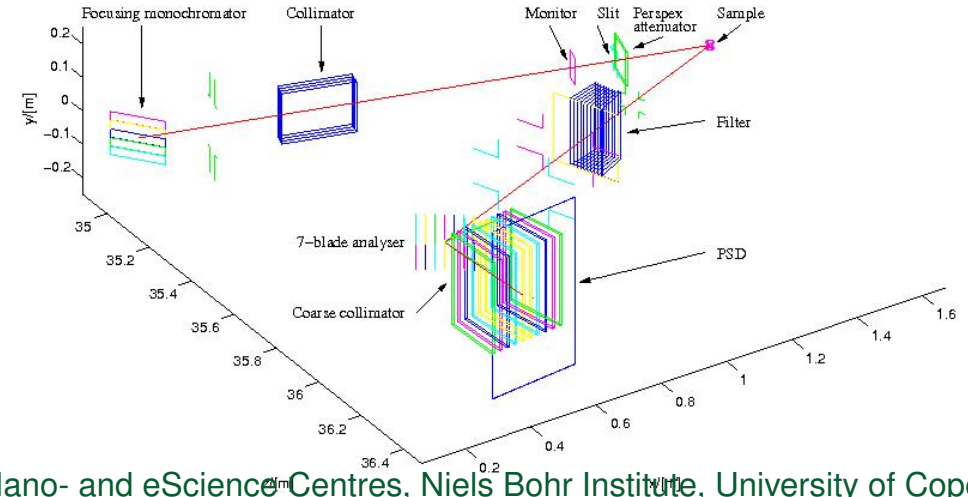

RITA-II TAS @ PSI with vertically focusing monochromator and multiblade analyser. Effective instrumental resolution and thereby the linewidth of a particular scan depends on

- Divergence of the beam before the monochromator: Size of source, geometry and m-values of guide elements
- Mosaicity of the monochromator
- Mosaicity of the analyser
- Geometrical factors: Sizes of components and distances between them
- Divergence of collimators
- Point-spread function of the position sensitive detector (PSD)
- Absolute energy of the incoming and scattered beam
- Sample parameters
  - shape/size (all samples including incoherent scatterer, powder, single-crystal)
  - particle size in sample (powder)
  - mosaicity and uncertainty in lattice parameters (single-crystal)

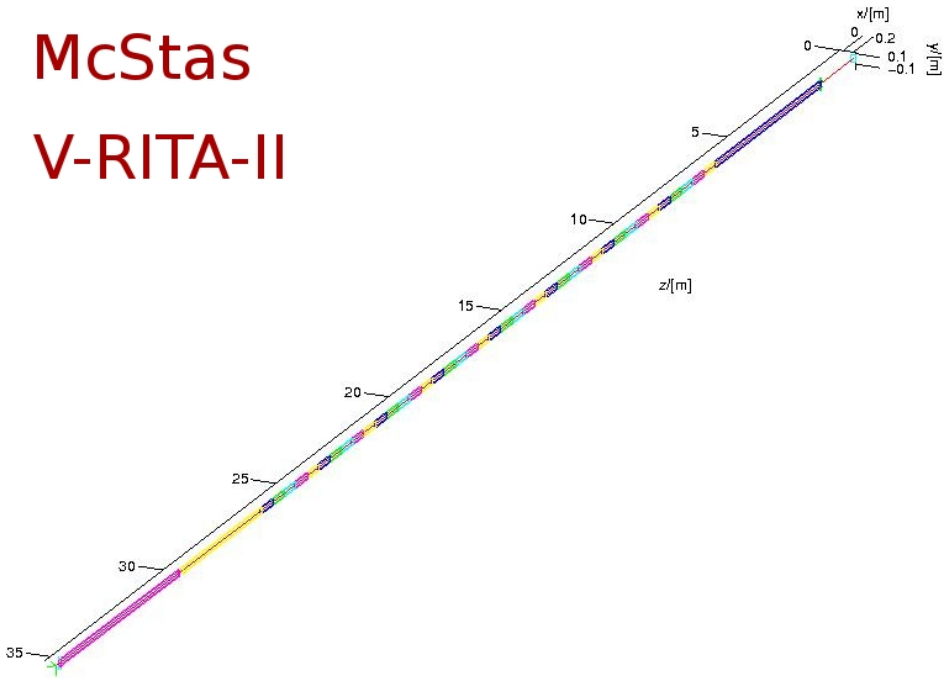

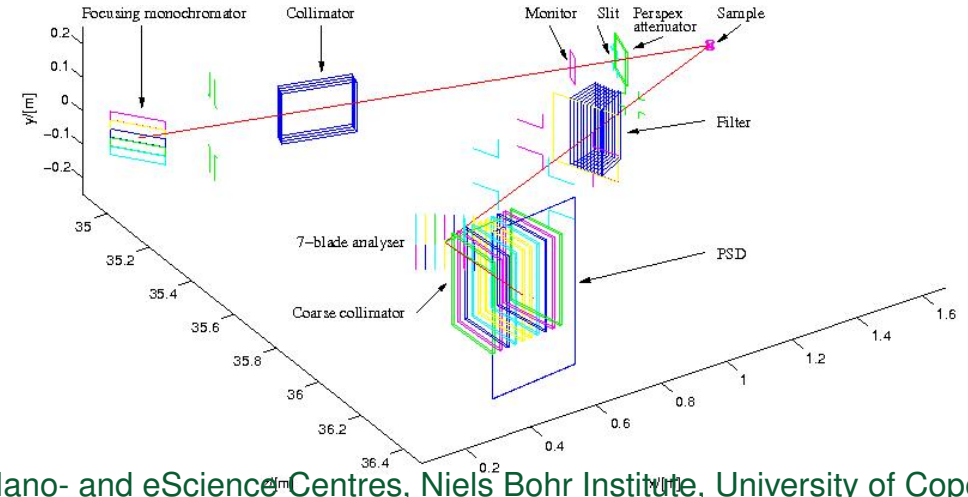

RITA-II TAS @ PSI with vertically focusing monochromator and multiblade analyser. Effective instrumental resolution and thereby the linewidth of a particular scan depends on

- Divergence of the beam before the monochromator: Size of source, geometry and m-values of guide elements
- Mosaicity of the monochromator
- Mosaicity of the analyser
- Geometrical factors: Sizes of components and distances between them
- Divergence of collimators
- Point-spread function of the position sensitive detector (PSD)
- Absolute energy of the incoming and scattered beam
- Sample parameters
  - shape/size (all samples including incoherent scatterer, powder, single-crystal)
  - particle size in sample (powder)
  - mosaicity and uncertainty in lattice parameters (single-crystal)

McStas

V-RITA-II

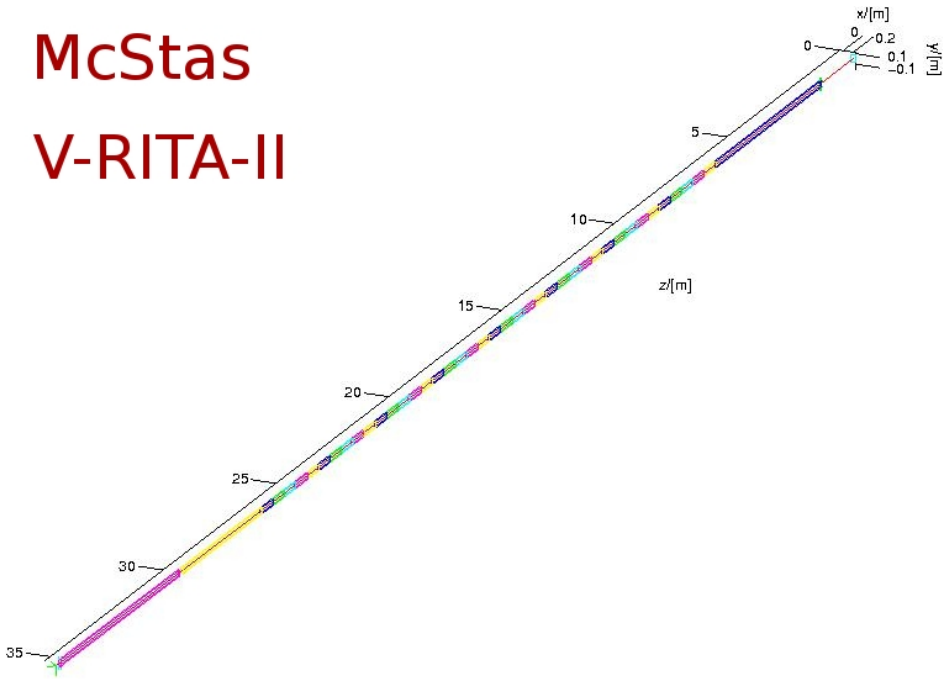

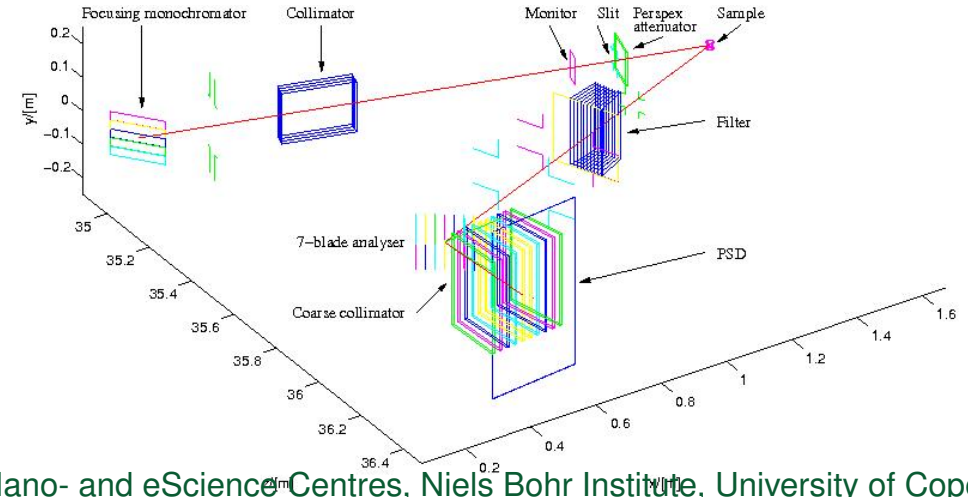

RITA-II TAS @ PSI with vertically focusing monochromator and multiblade analyser. Effective instrumental resolution and thereby the linewidth of a particular scan depends on

- Divergence of the beam before the monochromator: Size of source, geometry and m-values of guide elements
- Mosaicity of the monochromator
- Mosaicity of the analyser
- Geometrical factors: Sizes of components and distances between them
- Divergence of collimators
- Point-spread function of the position sensitive detector (PSD)
- Absolute energy of the incoming and scattered beam
- Sample parameters
  - shape/size (all samples including incoherent scatterer, powder, single-crystal)
  - particle size in sample (powder)
  - mosaicity and uncertainty in lattice parameters (single-crystal)

Vanadium sample

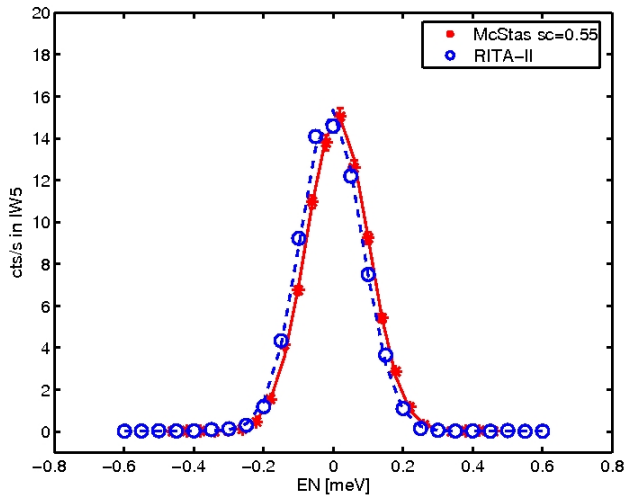

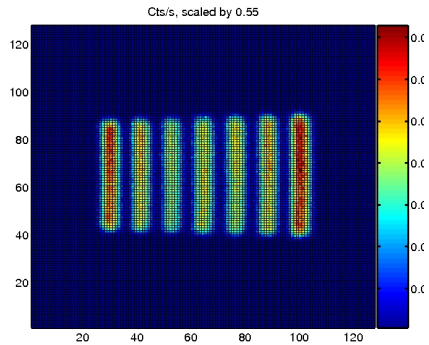

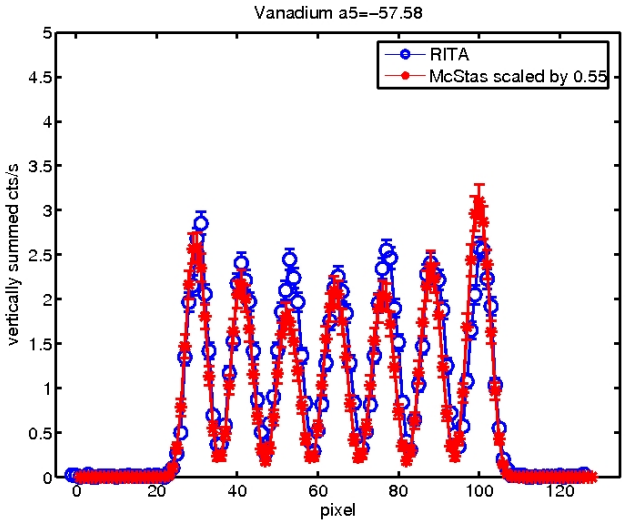

Powder sample

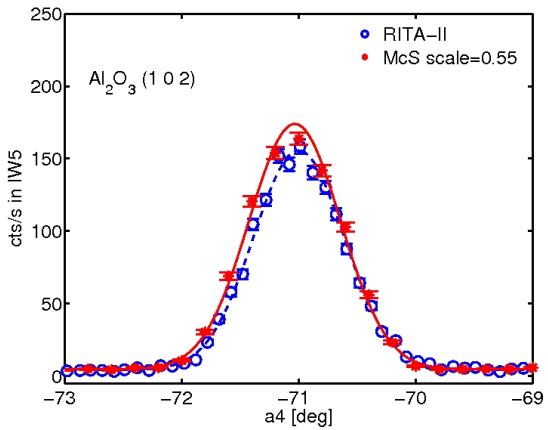

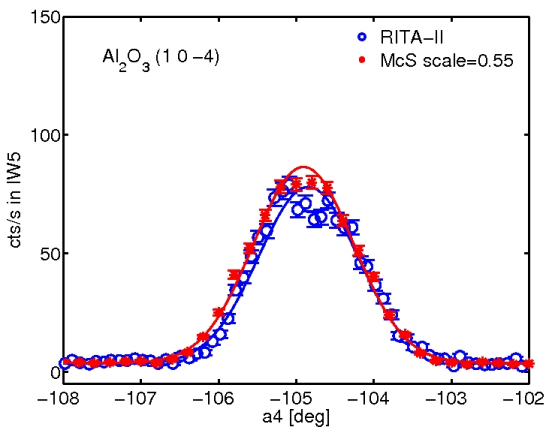

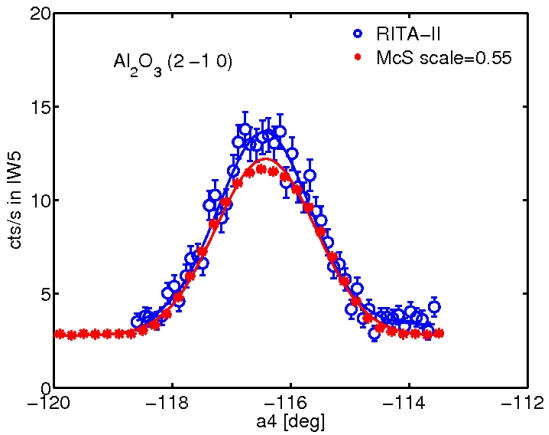

Virtual experiments - testing INSTRUMENT conclusion

#	Experiment	Year	Scale	Int	Linewidth
5	PowderN reflections (10-2)/(104)/(2-10)	2008	0.55	10%	2%
6	Elastic energy resolution (V sample)	2008	0.55	10%	2% (8%)
7	Ge single crystal	2008	0.55	10%	2 %
8	Ge wafer (perfect single crystal)	2008	0.55	10%	10%

- Intensity - Same scaling factor
  (due to efficiency of detector and taget neutron yield)
- Position - Within 0.05° corresp. small energy diff. of 0.1%
- Width - Mostly within 2%

Virtual experiments - testing INSTRUMENT conclusion

#	Experiment	Year	Scale	Int	Linewidth
5	PowderN reflections (10-2)/(104)/(2-10)	2008	0.55	10%	2%
6	Elastic energy resolution (V sample)	2008	0.55	10%	2% (8%)
7	Ge single crystal	2008	0.55	10%	2 %
8	Ge wafer (perfect single crystal)	2008	0.55	10%	10%

- Intensity - Same scaling factor
  (due to efficiency of detector and taget neutron yield)
- Position - Within 0.05° corresp. small energy diff. of 0.1%
- Width - Mostly within 2%

#	Experiment	Year	Scale	Int	Linewidth
5	PowderN reflections (10-2)/(104)/(2-10)	2008	0.55	10%	2%
6	Elastic energy resolution (V sample)	2008	0.55	10%	2% (8%)
7	Ge single crystal	2008	0.55	10%	2 %
8	Ge wafer (perfect single crystal)	2008	0.55	10%	10%

- Intensity - Same scaling factor
  (due to efficiency of detector and taget neutron yield)
- Position - Within 0.05° corresp. small energy diff. of 0.1%
- Width - Mostly within 2%

#	Experiment	Year	Scale	Int	Linewidth
5	PowderN reflections (10-2)/(104)/(2-10)	2008	0.55	10%	2%
6	Elastic energy resolution (V sample)	2008	0.55	10%	2% (8%)
7	Ge single crystal	2008	0.55	10%	2 %
8	Ge wafer (perfect single crystal)	2008	0.55	10%	10%

- Intensity - Same scaling factor
  (due to efficiency of detector and taget neutron yield)
- Position - Within 0.05° corresp. small energy diff. of 0.1%
- Width - Mostly within 2%

Real sample (LSCO+O)

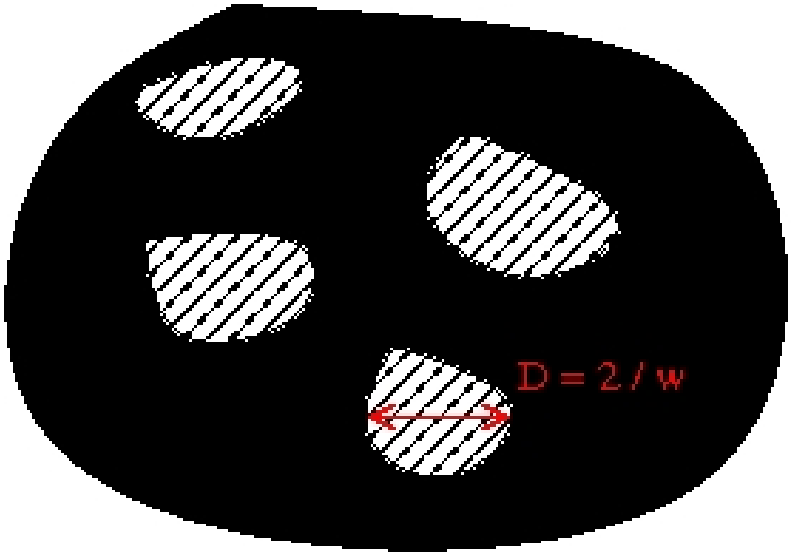

Virtual sample (LSCO)

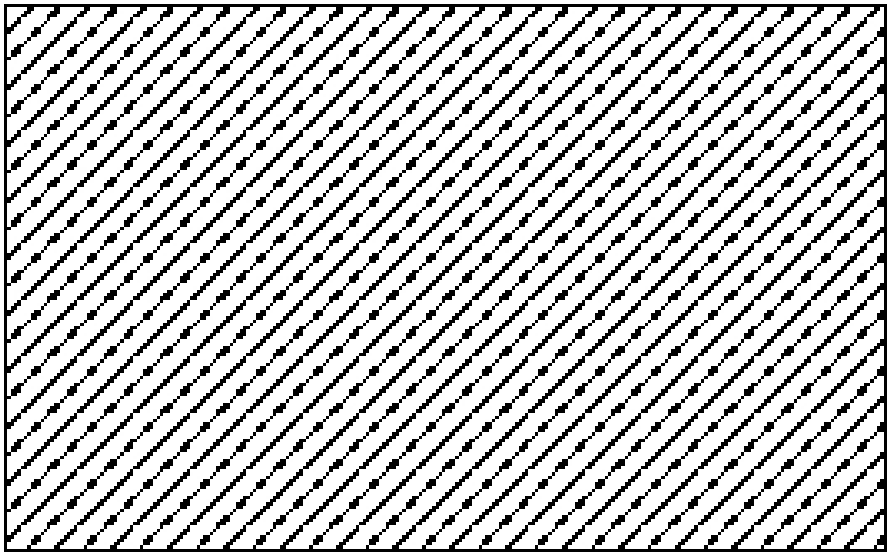

- Broadening due to stress/strain
- Broadening due to finite size effects

Stress/strain included in $\frac{\Delta d}{d}$ and mosaicity

Narrow peaks - instrumental width

Using the VE linewidth as 'homogeneous sample resolution', the deconvoluted width of experimental data is due to finite size effects!

Real sample (LSCO+O)

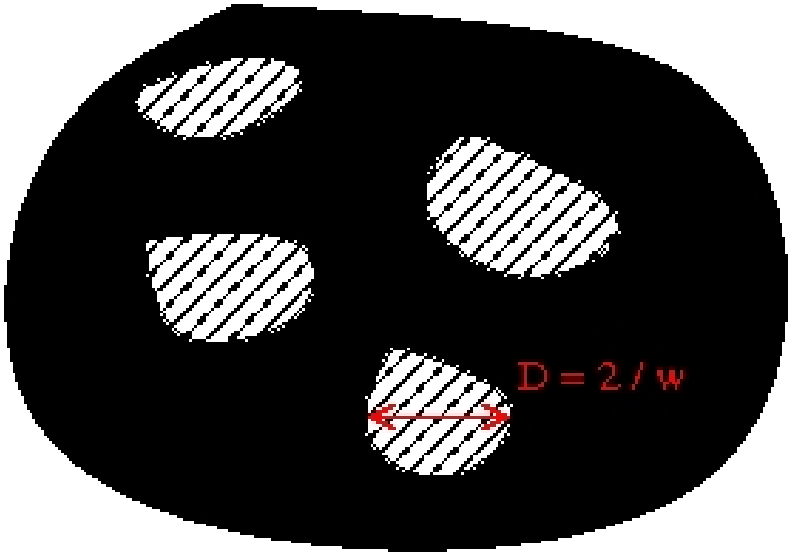

Virtual sample (LSCO)

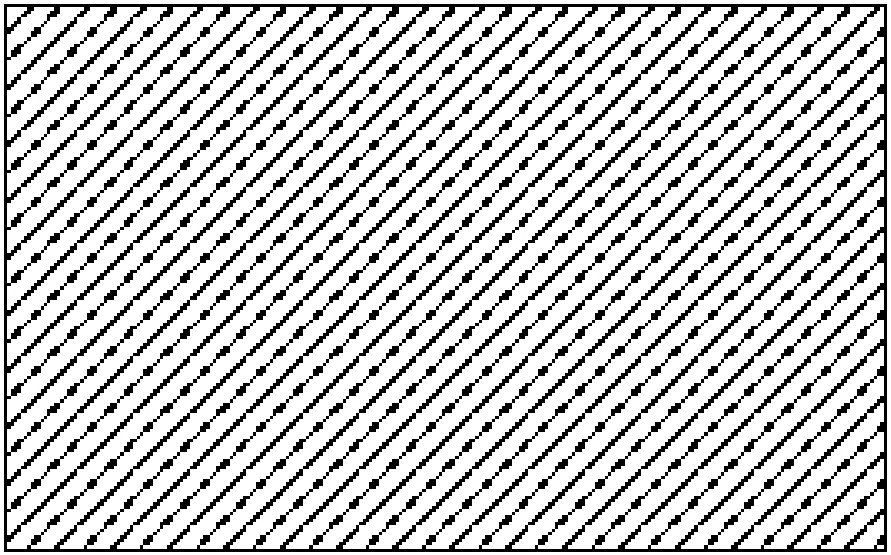

- Broadening due to stress/strain
- Broadening due to finite size effects

Stress/strain included in $\frac{\Delta d}{d}$ and mosaicity

Narrow peaks - instrumental width

Using the VE linewidth as 'homogeneous sample resolution', the deconvoluted width of experimental data is due to finite size effects!

Real sample (LSCO+O)

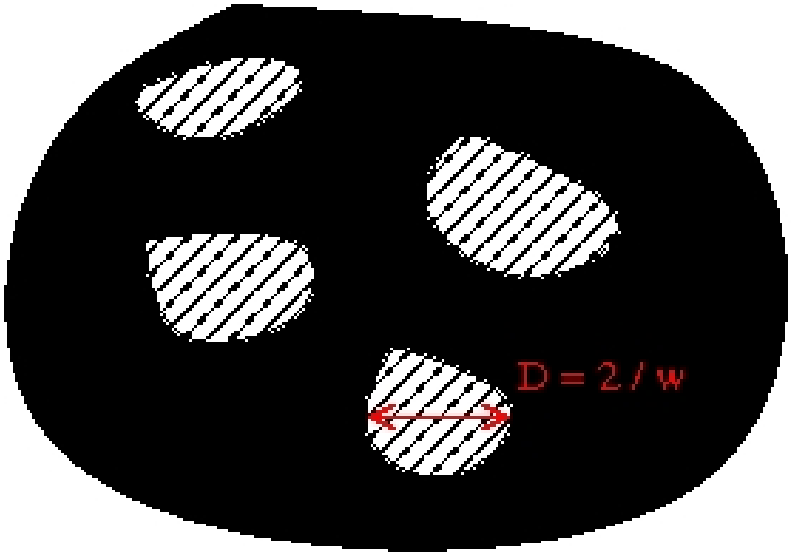

Virtual sample (LSCO)

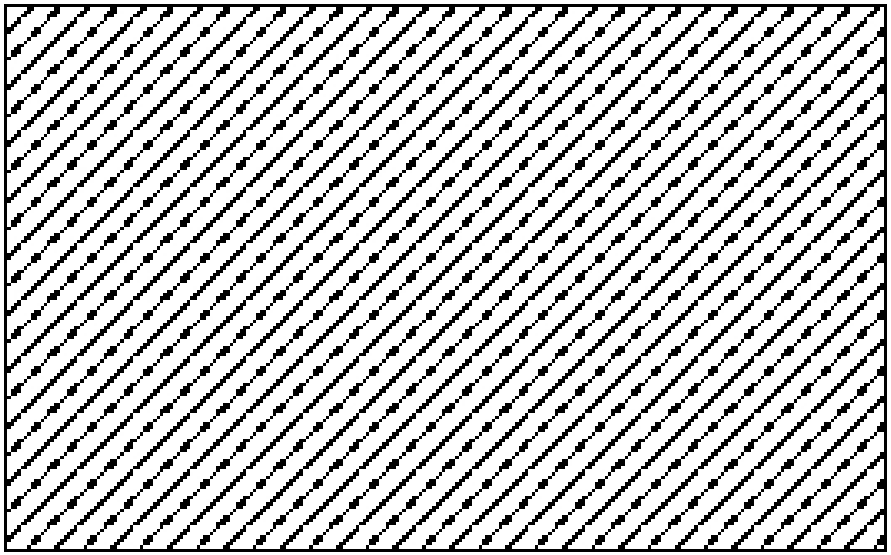

- Broadening due to stress/strain
- Broadening due to finite size effects

Stress/strain included in $\frac{\Delta d}{d}$ and mosaicity

Narrow peaks - instrumental width

Using the VE linewidth as 'homogeneous sample resolution', the deconvoluted width of experimental data is due to finite size effects!

Real sample (LSCO+O)

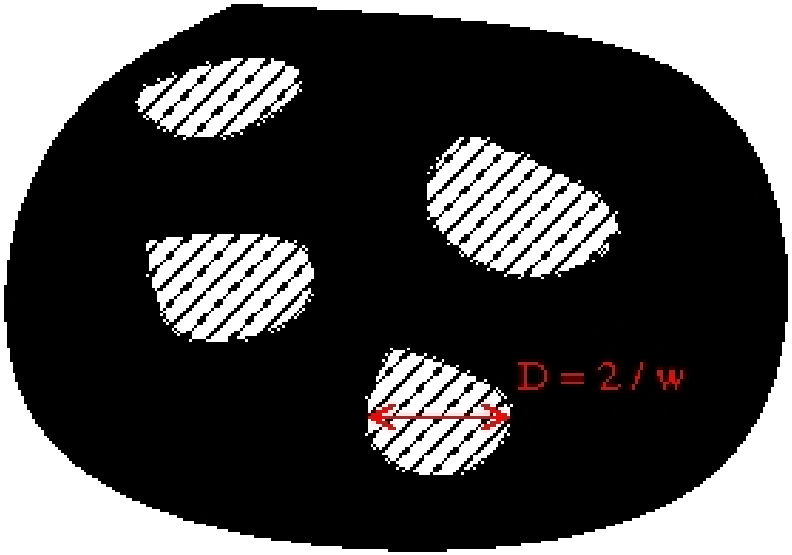

- Broadening due to stress/strain
- Broadening due to finite size effects

Virtual sample (LSCO)

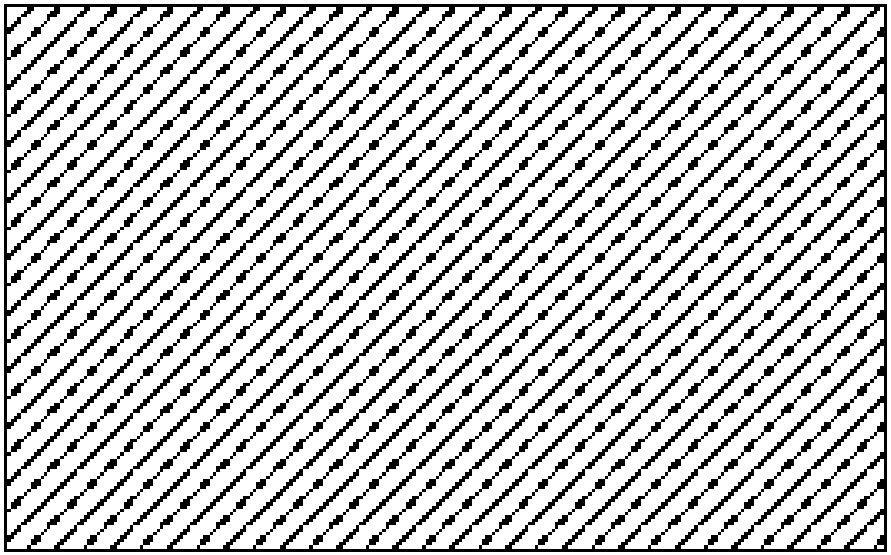

Stress/strain included in $\frac{\Delta d}{d}$ and mosaicity

Narrow peaks - instrumental width

Using the VE linewidth as 'homogeneous sample resolution', the deconvoluted width of experimental data is due to finite size effects!

Real sample (LSCO+O)

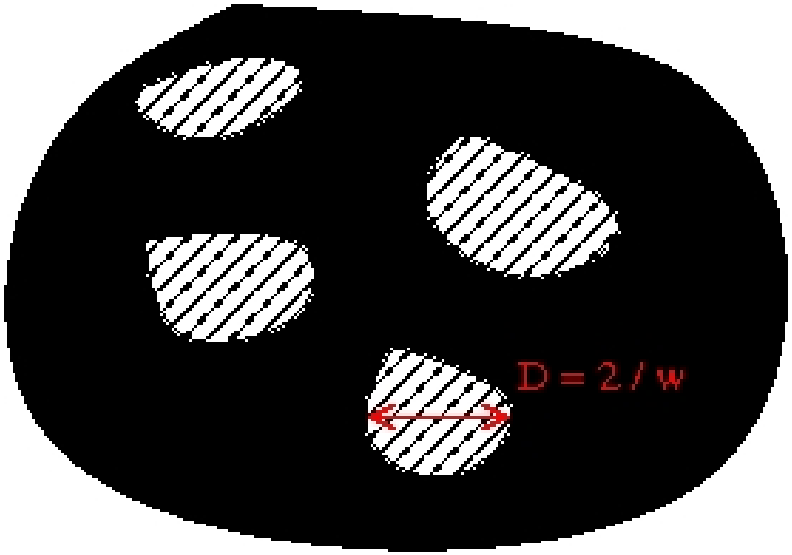

- Broadening due to stress/strain
- Broadening due to finite size effects

Virtual sample (LSCO)

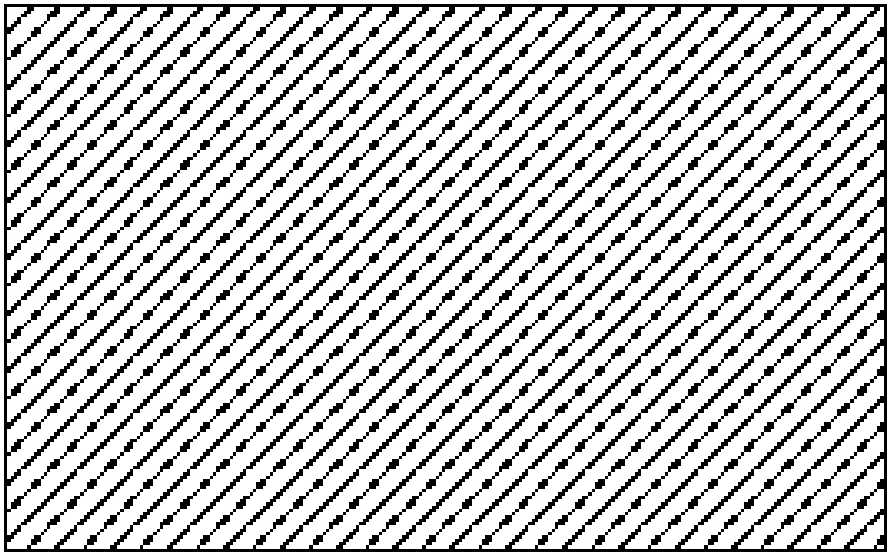

Stress/strain included in $\frac{\Delta d}{d}$ and mosaicity

Narrow peaks - instrumental width

Using the VE linewidth as 'homogeneous sample resolution', the deconvoluted width of experimental data is due to finite size effects!

Real sample (LSCO+O)

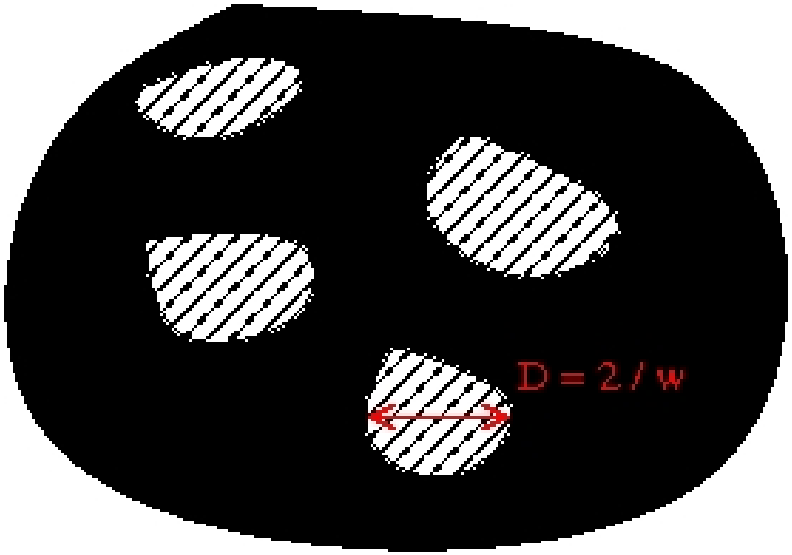

Virtual sample (LSCO)

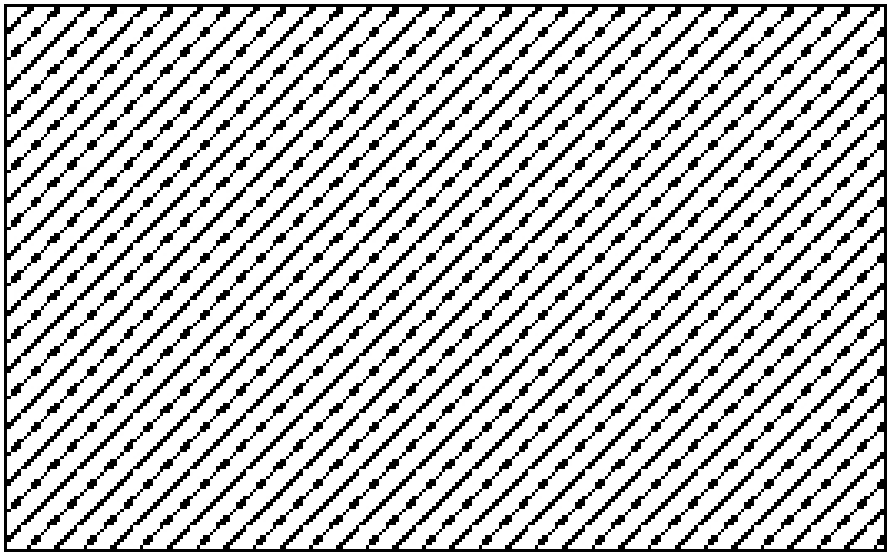

- Broadening due to stress/strain — Stress/strain included in $\frac{\Delta d}{d}$ and mosaicity
- Broadening due to finite size effects — Narrow peaks - instrumental width

Using the VE linewidth as 'homogeneous sample resolution', the deconvoluted width of experimental data is due to finite size effects!

Real sample (LSCO+O)

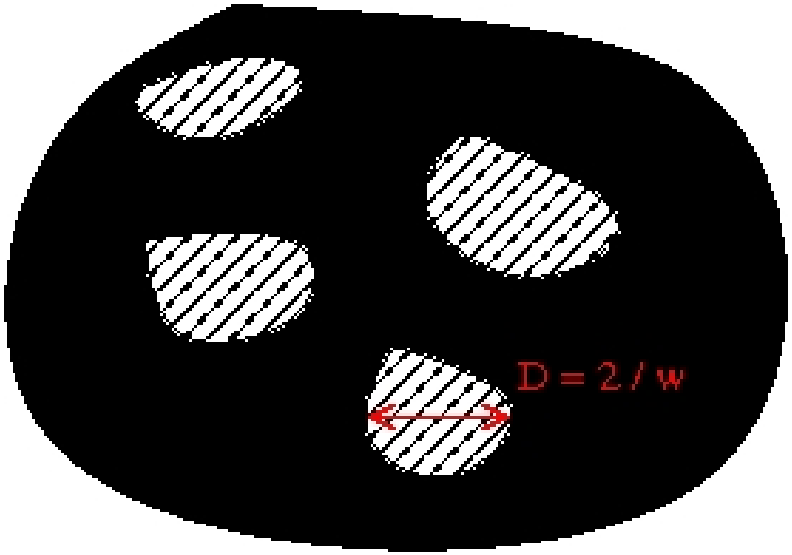

Virtual sample (LSCO)

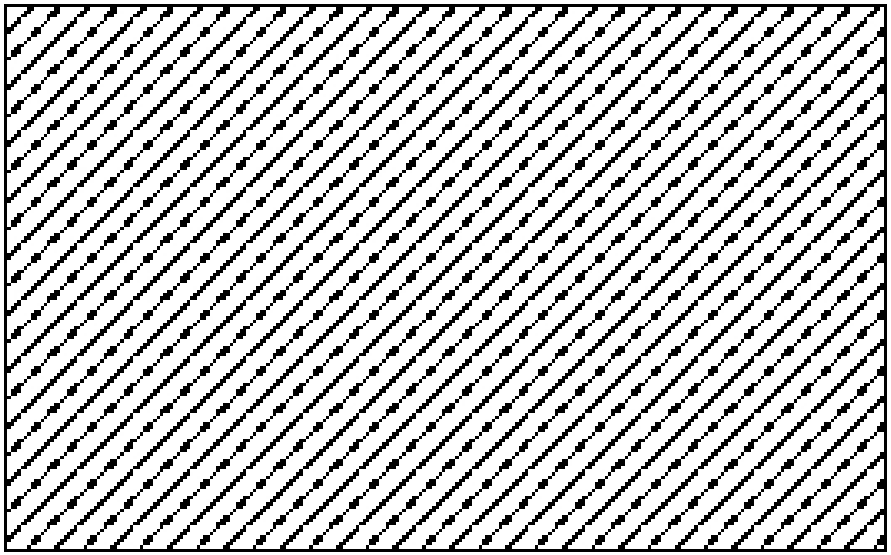

- Broadening due to stress/strain — Stress/strain included in $\frac{\Delta d}{d}$ and mosaicity
- Broadening due to finite size effects — Narrow peaks - instrumental width

Using the VE linewidth as 'homogeneous sample resolution', the deconvoluted width of experimental data is due to finite size effects!

Virtual experiments - adjusting SINGLE-CRYSTAL

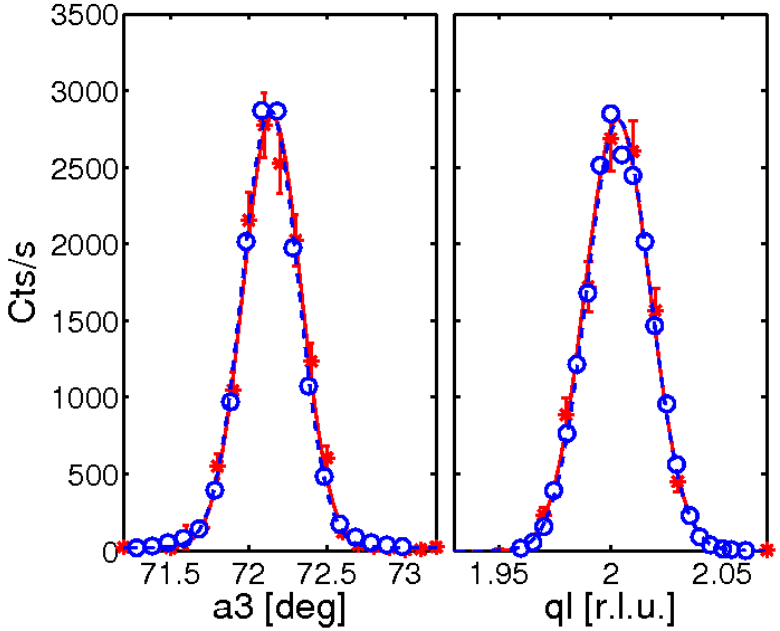

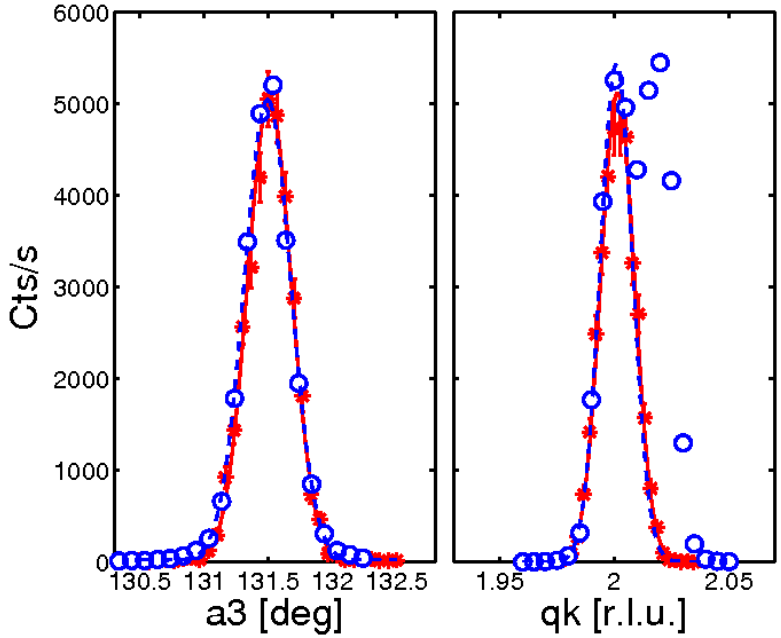

- McStas ○ RITA-II
  - Fundamental reflections
  - Assume peaks instr. res.
  - Use to set mosaicity and $\frac{\Delta d}{d}$ of virtual sample
  - Simulated (resolution) width agrees within 5% of measured

Virtual experiments - adjusting SINGLE-CRYSTAL

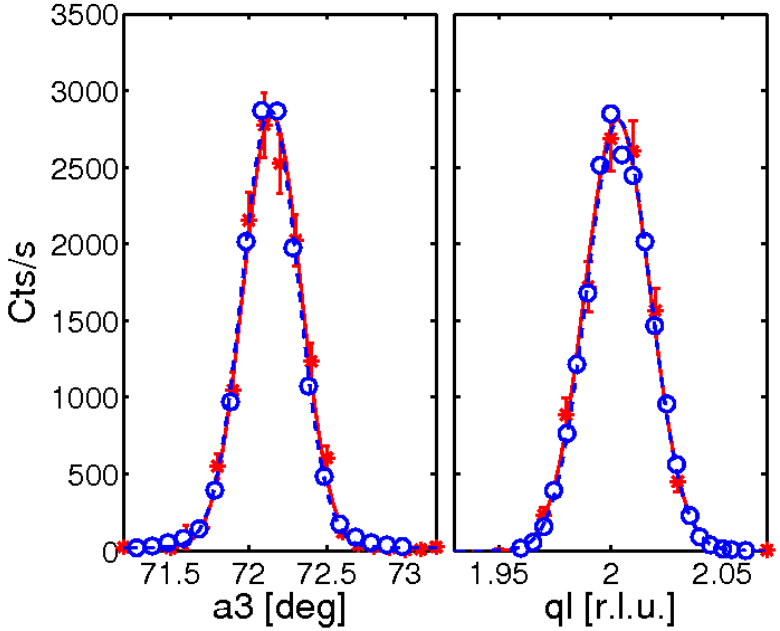

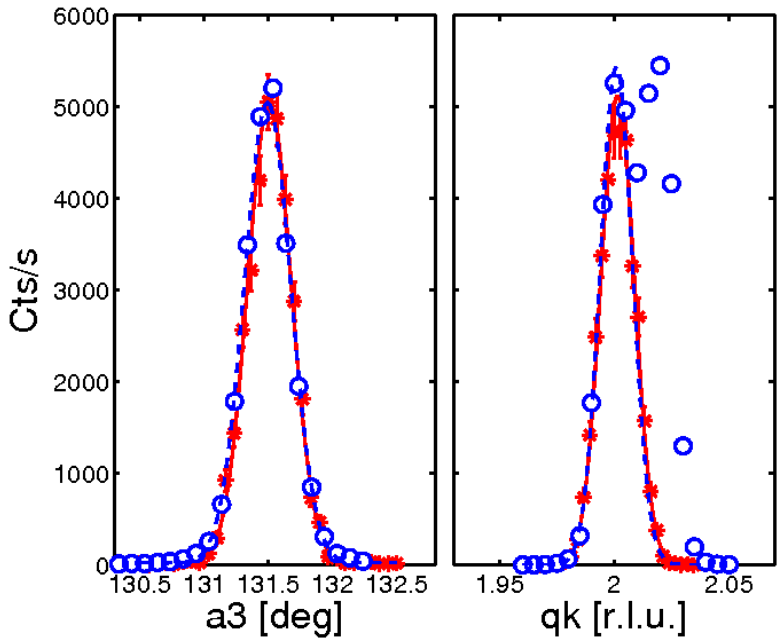

- McStas ○ RITA-II
  - Fundamental reflections
  - Assume peaks instr. res.
  - Use to set mosaicity and $\frac{\Delta d}{d}$ of virtual sample
  - Simulated (resolution) width agrees within 5% of measured

Virtual experiments - adjusting SINGLE-CRYSTAL

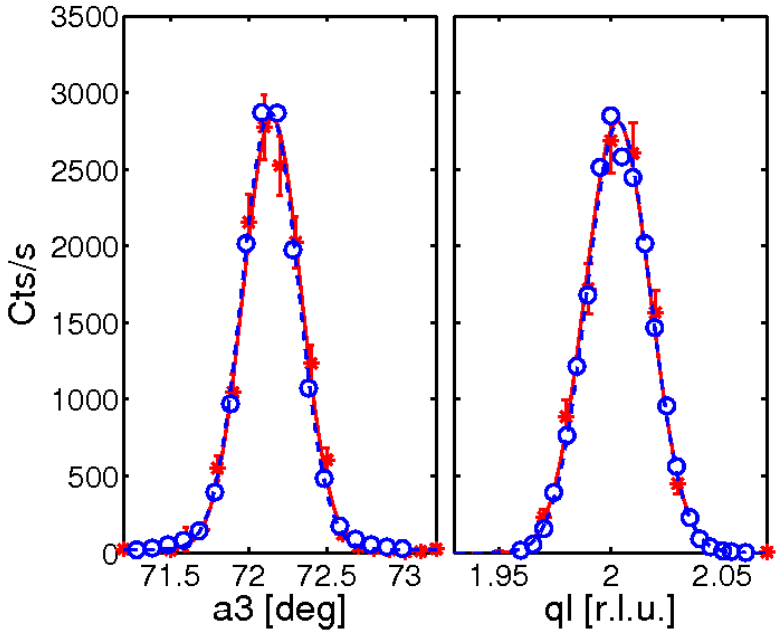

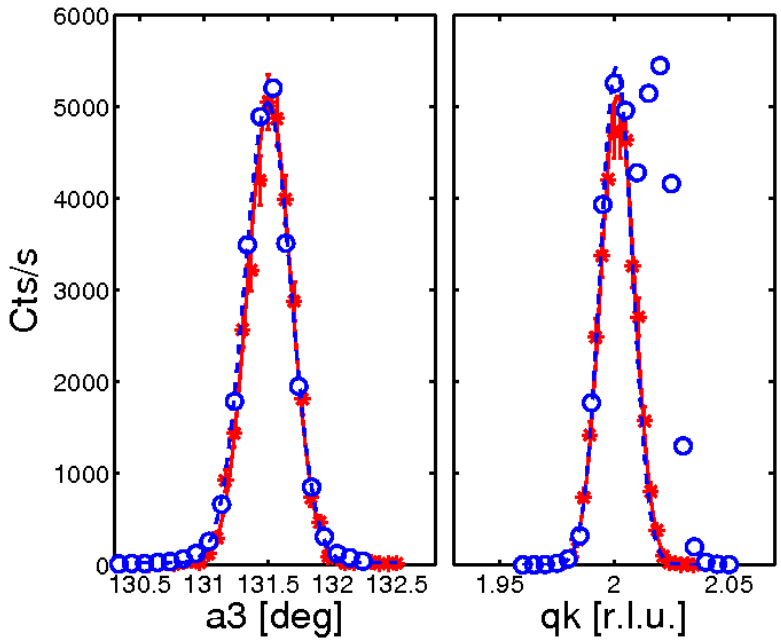

- McStas ○ RITA-II
  - Fundamental reflections
  - Assume peaks instr. res.
  - Use to set mosaicity and $\frac{\Delta d}{d}$ of virtual sample
  - Simulated (resolution) width agrees within 5% of measured

Virtual experiments - adjusting SINGLE-CRYSTAL

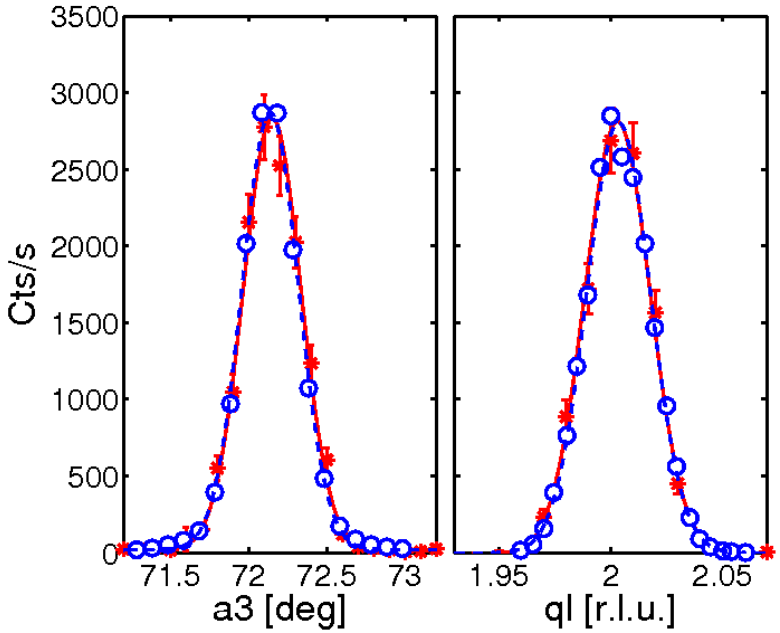

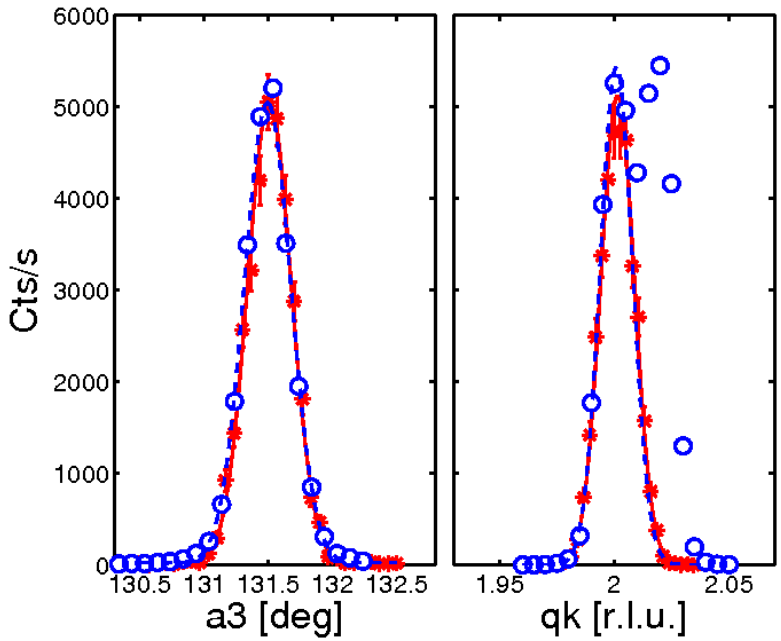

- McStas ○ RITA-II
  - Fundamental reflections
  - Assume peaks instr. res.
  - Use to set mosaicity and $\frac{\Delta d}{d}$ of virtual sample
  - Simulated (resolution) width agrees within 5% of measured

#	Experiment	Scale	Int	Line width
9	LSCO+O x=0 (fund. *KL* reflections)	0.3	20%	5%
10	LSCO+O x=0.04 (fund. *KL* reflections)	0.4	5%	5%
11	LSCO+O x=0.065 (fund. *KL* reflections)	0.55	20%	5%
12	LSCO+O x=0.09 (fund. *HK* reflections)	0.7	10%	5%
14	LSCO+O x=0.09 (fund. *KL* reflections)	1.5	10%	5%

- Intensity - scale influenced by sample geometry (and varying n.y. from source over the years)
- Position - within 0.2% (when adjusted in physical exp.)
- Width - within 5%

#	Experiment	Scale	Int	Line width
9	LSCO+O x=0 (fund. *KL* reflections)	0.3	20%	5%
10	LSCO+O x=0.04 (fund. *KL* reflections)	0.4	5%	5%
11	LSCO+O x=0.065 (fund. *KL* reflections)	0.55	20%	5%
12	LSCO+O x=0.09 (fund. *HK* reflections)	0.7	10%	5%
14	LSCO+O x=0.09 (fund. *KL* reflections)	1.5	10%	5%

- Intensity - scale influenced by sample geometry (and varying n.y. from source over the years)
- Position - within 0.2% (when adjusted in physical exp.)
- Width - within 5%

#	Experiment	Scale	Int	Line width
9	LSCO+O x=0 (fund. *KL* reflections)	0.3	20%	5%
10	LSCO+O x=0.04 (fund. *KL* reflections)	0.4	5%	5%
11	LSCO+O x=0.065 (fund. *KL* reflections)	0.55	20%	5%
12	LSCO+O x=0.09 (fund. *HK* reflections)	0.7	10%	5%
14	LSCO+O x=0.09 (fund. *KL* reflections)	1.5	10%	5%

- Intensity - scale influenced by sample geometry (and varying n.y. from source over the years)
- Position - within 0.2% (when adjusted in physical exp.)
- Width - within 5%

#	Experiment	Scale	Int	Line width
9	LSCO+O x=0 (fund. *KL* reflections)	0.3	20%	5%
10	LSCO+O x=0.04 (fund. *KL* reflections)	0.4	5%	5%
11	LSCO+O x=0.065 (fund. *KL* reflections)	0.55	20%	5%
12	LSCO+O x=0.09 (fund. *HK* reflections)	0.7	10%	5%
14	LSCO+O x=0.09 (fund. *KL* reflections)	1.5	10%	5%

- Intensity - scale influenced by sample geometry (and varying n.y. from source over the years)
- Position - within 0.2% (when adjusted in physical exp.)
- Width - within 5%

x=0.09

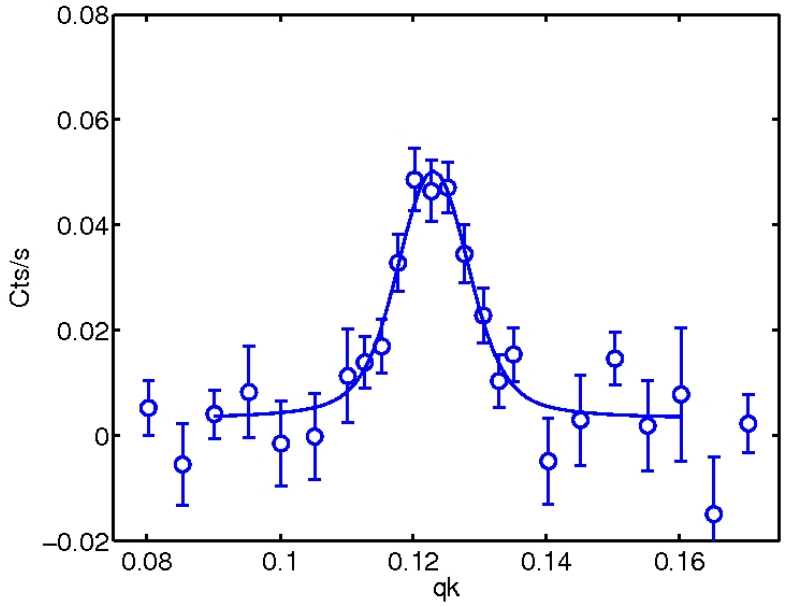

IC AFM broadened:

Fit to Voigt

w^L =0.06(2) nm^{-1} $\Rightarrow$

Corr.= $\frac{2}{w^L}$ = 34± 13 nm

Fit to Gaussian

$w = \sqrt{w_m^2 - w_r^2}$

w^G=0.10 nm^{-1} $\Rightarrow$

$D = \frac{2\pi}{w^G} \sim 61 \pm 14$ nm

- The IC AFM peak is narrow and close to resolution limited...

  but effects larger than 10% are observable by McStas VE

x=0.09

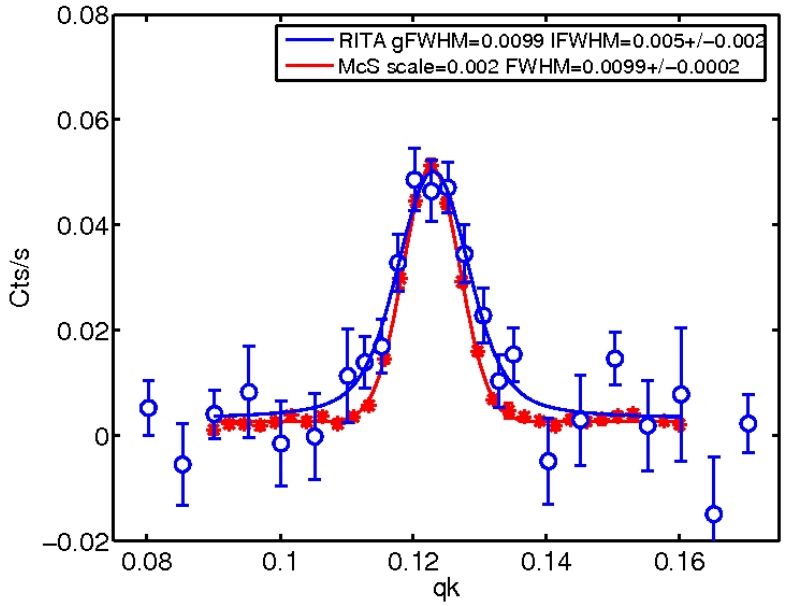

IC AFM broadened:

Fit to Voigt

w^L =0.06(2) nm^{-1} $\Rightarrow$

Corr.= $\frac{2}{w^L}$ = 34± 13 nm

Fit to Gaussian

$w = \sqrt{w_m^2 - w_r^2}$

w^G=0.10 nm^{-1} $\Rightarrow$

$D = \frac{2\pi}{w^G} \sim$ 61±14 nm

- The IC AFM peak is narrow and close to resolution limited... but effects larger than 10% are observable by McStas VE

x=0.09

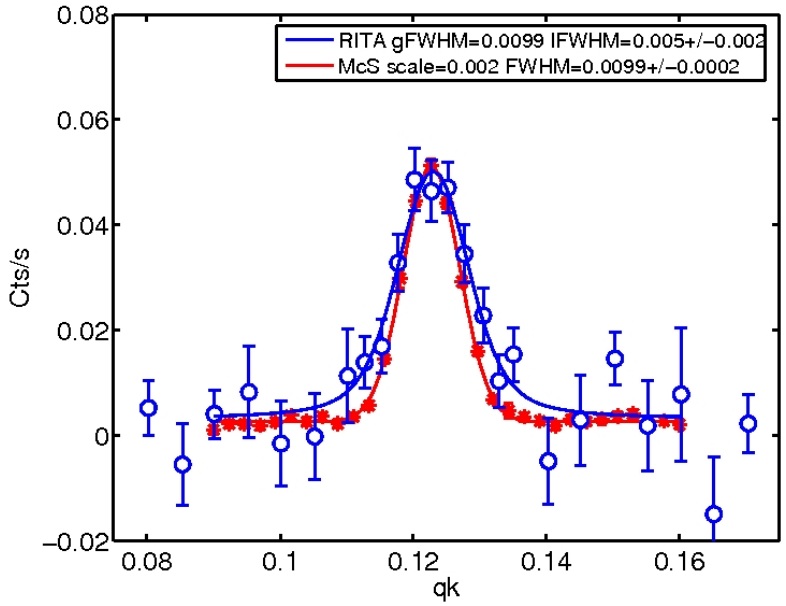

IC AFM broadened:

Fit to Voigt

w^L =0.06(2) nm^{-1} $\Rightarrow$

Corr.= $\frac{2}{w^L}$ = 34± 13 nm

Fit to Gaussian

$w = \sqrt{w_m^2 - w_r^2}$

w^G=0.10 nm^{-1} $\Rightarrow$

$D = \frac{2\pi}{w^G} \sim$ 61±14 nm

- The IC AFM peak is narrow and close to resolution limited... but effects larger than 10% are observable by McStas VE

x=0.04

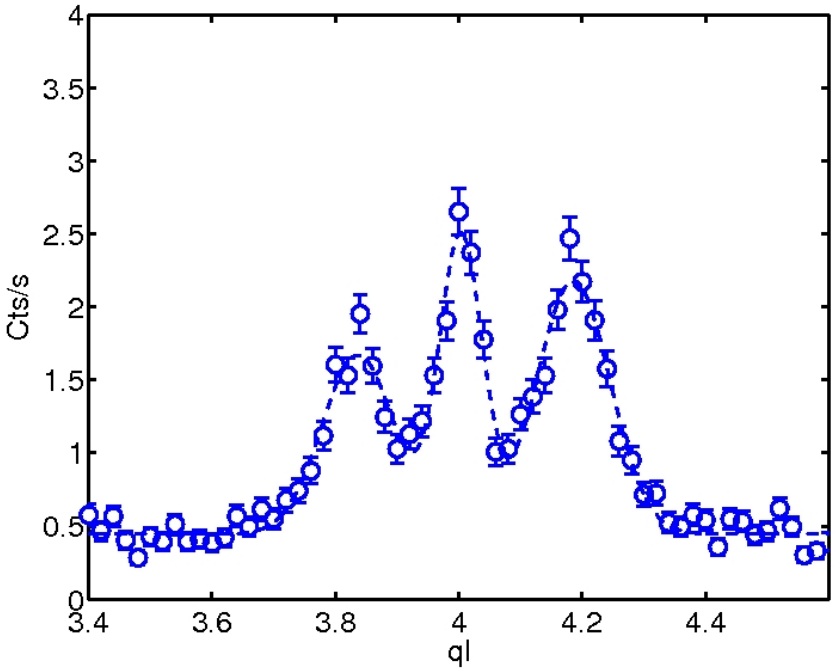

Bragg peak broadened:
w^G=0.34 nm^{-1}
Domain size $\frac{2\pi}{w^G} \sim 19 \pm 3$ nm

Superstructure broadened:
w^G=0.64 nm^{-1}
Domain size $\frac{2\pi}{w^G} \sim 10 \pm 1$ nm

- Mcstas VE is a useful tool when there is no instrumentally resolved peak in the vicinity

x=0.04

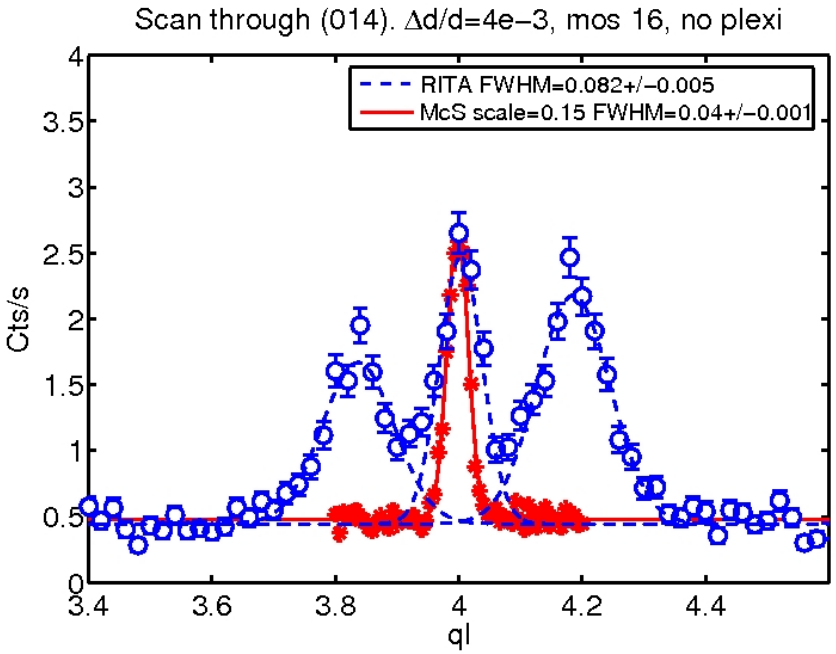

Bragg peak broadened:
w^G=0.34 nm^{-1}
Domain size $\frac{2\pi}{w^G} \sim 19 \pm 3$ nm

Superstructure broadened:
w^G=0.64 nm^{-1}
Domain size $\frac{2\pi}{w^G} \sim 10 \pm 1$ nm

- Mcstas VE is a useful tool when there is no instrumentally resolved peak in the vicinity

x=0.04

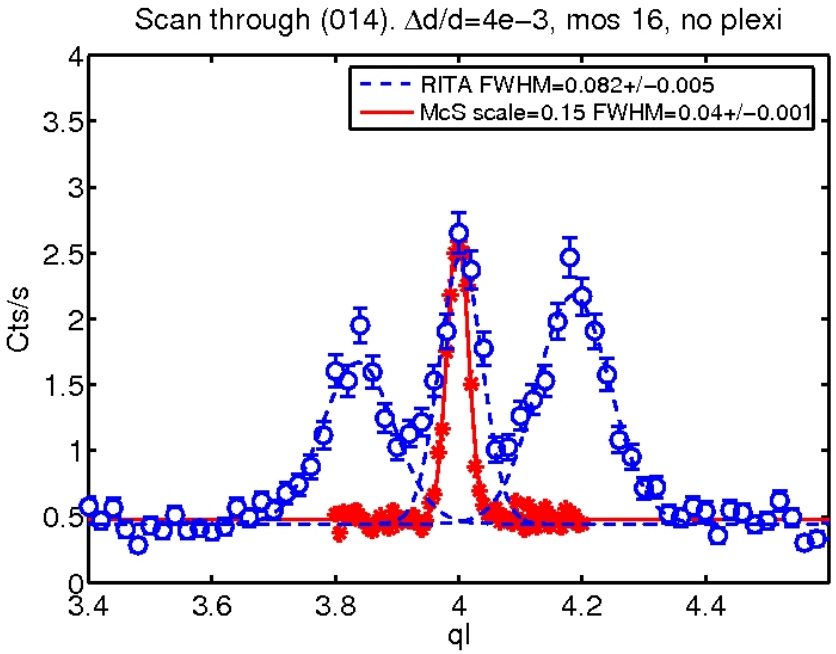

Bragg peak broadened:
w^G=0.34 nm^{-1}
Domain size $\frac{2\pi}{w^G} \sim 19 \pm 3$ nm

Superstructure broadened:
w^G=0.64 nm^{-1}
Domain size $\frac{2\pi}{w^G} \sim 10 \pm 1$ nm

- Mcstas VE is a useful tool when there is no instrumentally resolved peak in the vicinity

x=0.04

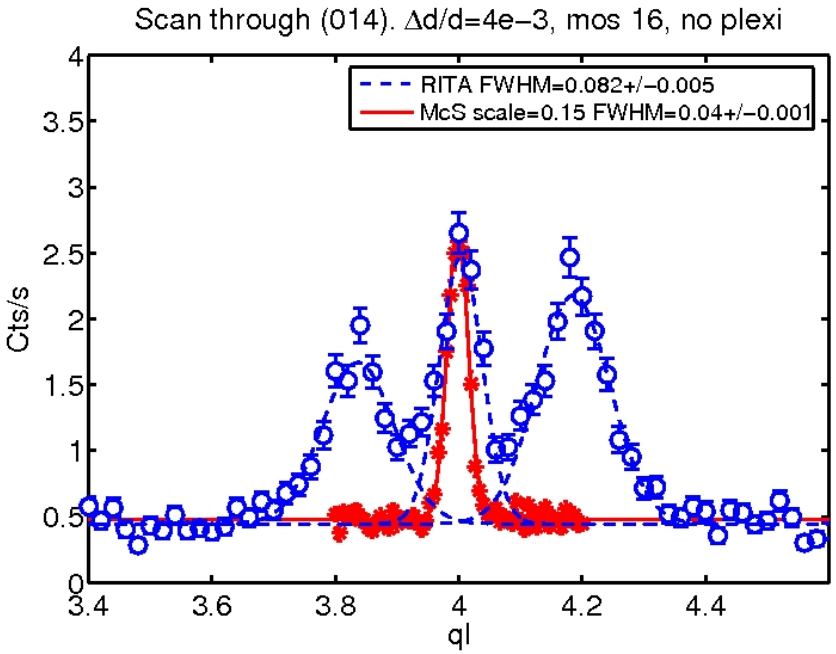

Bragg peak broadened:
w^G=0.34 nm^{-1}
Domain size $\frac{2\pi}{w^G} \sim 19 \pm 3$ nm

Superstructure broadened:
w^G=0.64 nm^{-1}
Domain size $\frac{2\pi}{w^G} \sim 10 \pm 1$ nm

- Mcstas VE is a useful tool when there is no instrumentally resolved peak in the vicinity

Conclusion on the VE with RITA-II

- McStas VE can be used to obtain detailed knowledge of the resolution in specific instrument configurations
- McStas VE can be used to deconvolute finite size peak width from experimental data
- McStas VE can be used to set lower and upper limit of domainsize. Even at several hundred Å.

Want to know more? Take at look at Udby et al. NIMA **634** (2011)

Conclusion on the VE with RITA-II

- McStas VE can be used to obtain detailed knowledge of the resolution in specific instrument configurations
- McStas VE can be used to deconvolute finite size peak width from experimental data
- McStas VE can be used to set lower and upper limit of domainsize. Even at several hundred Å.

Want to know more? Take at look at Udby et al. NIMA **634** (2011)

Conclusion on the VE with RITA-II

- McStas VE can be used to obtain detailed knowledge of the resolution in specific instrument configurations
- McStas VE can be used to deconvolute finite size peak width from experimental data
- McStas VE can be used to set lower and upper limit of domainsize. Even at several hundred Å.

Want to know more? Take at look at Udby et al. NIMA **634** (2011)

Conclusion on the VE with RITA-II

- McStas VE can be used to obtain detailed knowledge of the resolution in specific instrument configurations
- McStas VE can be used to deconvolute finite size peak width from experimental data
- McStas VE can be used to set lower and upper limit of domainsize. Even at several hundred Å.

Want to know more? Take at look at Udby et al. NIMA **634** (2011)

Conclusion on the VE with RITA-II

- McStas VE can be used to obtain detailed knowledge of the resolution in specific instrument configurations
- McStas VE can be used to deconvolute finite size peak width from experimental data
- McStas VE can be used to set lower and upper limit of domainsize. Even at several hundred Å.

Want to know more? Take at look at Udby et al. NIMA **634** (2011)

I would like to thank my coworkers:

- McStas VE: Kim Lefmann(UCPH/ESS-DK),
  Peter K. Willendrup (Risø DTU),
  Erik Knudsen(Risø DTU), Emmanuel Farhi (ILL)
- Real Experiments:
  Christof Niedermayer (PSI), Niels H. Andersen (Risø DTU)
- Samples: Barret O. Wells (UCONN), Hashini E. Mohottala(UCONN),
  Samuel B. Emery (UCONN), F.-C. Chou (TAIWAN)

Outline

- How do I implement magnetic fields in McStas?
- SESANS - the Delft version
- Virtual vs real experiments with refracting prism

Outline

- How do I implement magnetic fields in McStas?
- SESANS - the Delft version
- Virtual vs real experiments with refracting prism

Outline

- How do I implement magnetic fields in McStas?
- SESANS - the Delft version
- Virtual vs real experiments with refracting prism

Outline

- How do I implement magnetic fields in McStas?
- SESANS - the Delft version
- Virtual vs real experiments with refracting prism

Example Entries I in Instrument file

A circular source (radius 10 cm) aimed at a guide opening 1 m downstream, with main wavelength `Lambda` ± `DL`

```
COMPONENT source = Source_simple(
  radius = 0.01, dist = 1.0,
  focus_xw = 21.5e-3, focus_yh = 80e-3,
  lambda0 = Lambda,dlambda = DL)
AT (0, 0, 0) RELATIVE Origin
```

Example Entries II in Instrument file

Entry into a region with nonzero magnetic field $\mathbf{B} = (0, B_y, 0)$.
Field starts 2 mm after the component `something`

```
COMPONENT guide_field=Pol_simpleBfield(
  xwidth=0.5,yheight=0.3,
  Bx=0, By=By, Bz=0,
  fieldFunction=const_magnetic_field)
AT (0,0,0.002) RELATIVE something
```

... and ends 2.025 m thereafter

```
COMPONENT guide_field_stop=Pol_simpleBfield_stop(
magnet_comp_stop=guide_field)
AT(0,0,2.025) RELATIVE guide_field
```

Example Entries II in Instrument file

Entry into a region with nonzero magnetic field $\mathbf{B} = (0, B_y, 0)$.
Field starts 2 mm after the component `something`

```
COMPONENT guide_field=Pol_simpleBfield(
  xwidth=0.5,yheight=0.3,
  Bx=0, By=By, Bz=0,
  fieldFunction=const_magnetic_field)
AT (0,0,0.002) RELATIVE something
```

... and ends 2.025 m thereafter

```
COMPONENT guide_field_stop=Pol_simpleBfield_stop(
magnet_comp_stop=guide_field)
AT(0,0,2.025) RELATIVE guide_field
```

How does precession work in McStas


```
while n_t < t_target do
    store neutron;
    sample magnetic field: B_1 = B(n_x, n_y, n_z, n_t);
    propagate neutron: δt(< Δt);
    sample magnetic field: B_2 = B(n_x, n_y, n_z, n_t);
    if |B_1 − B_2| > δ_threshold then
        restore neutron;
        δt := δt/2;
        propagate neutron: δt(< Δt);
        sample magnetic field: B_2 = B(n_x, n_y, n_z, n_t);
    else
        precess polarization: P by ω around (B_1+B_2)/2;
```

How does precession work in McStas


```
while n_t < t_target do
    store neutron;
    sample magnetic field: B_1 = B(n_x, n_y, n_z, n_t);
    propagate neutron: δt(< Δt);
    sample magnetic field: B_2 = B(n_x, n_y, n_z, n_t);
    if |B_1 − B_2| > δ_threshold then
        restore neutron;
        δt := δt/2;
        propagate neutron: δt(< Δt);
        sample magnetic field: B_2 = B(n_x, n_y, n_z, n_t);
    else
        precess polarization: P by ω around (B_1+B_2)/2;
```

```
while n_t < t_target do
    store neutron;
    sample initial magnetic field: B_1 = B(n_x, n_y, n_z, n_t);
    rotate to local coordinate system so B_1 is along z-axis;
    calculate S(δt) by Romberg Integration;
    propagate neutron: δt(< Δt);
    sample magnetic field: B_2 = B(n_x, n_y, n_z, n_t);
    while t_rk < δt do
        make table of S(t_rk) versus B(t_rk) from Romberg Integration to
        be used in the Runge-Kutta procedure;
    obtain start values for θ and φ;
    solve differential equations for θ(S) and φ(S) by Runge-Kutta
    Cash-Karp;
    update P according to θ(S) and φ(S);
```

How does precession work in McStas


```
while n_t < t_target do
    store neutron;
    sample magnetic field: B_1 = B(n_x, n_y, n_z, n_t);
    propagate neutron: δt(< Δt);
    sample magnetic field: B_2 = B(n_x, n_y, n_z, n_t);
    if |B_1 − B_2| > δ_threshold then
        restore neutron;
        δt := δt/2;
        propagate neutron: δt(< Δt);
        sample magnetic field: B_2 = B(n_x, n_y, n_z, n_t);
    else
        precess polarization: P by ω around (B_1+B_2)/2;
```

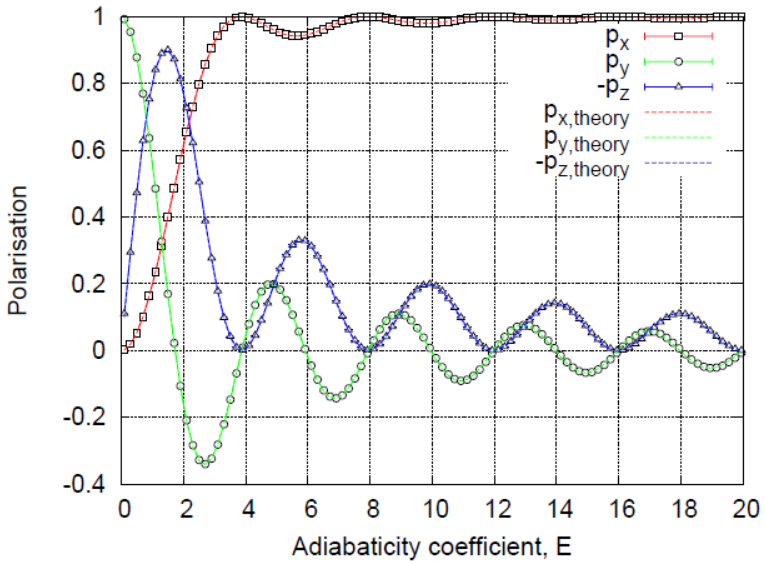

Adiabacity coefficient $E = -2\gamma B \Delta t/\pi$, where $\Delta t = m_n \lambda L/h$

How does precession work in McStas


```
while n_t < t_target do
    store neutron;
    sample magnetic field: B_1 = B(n_x, n_y, n_z, n_t);
    propagate neutron: δt(< Δt);
    sample magnetic field: B_2 = B(n_x, n_y, n_z, n_t);
    if |B_1 − B_2| > δ_threshold then
        restore neutron;
        δt := δt/2;
        propagate neutron: δt(< Δt);
        sample magnetic field: B_2 = B(n_x, n_y, n_z, n_t);
    else
        precess polarization: P by ω around (B_1+B_2)/2;
```

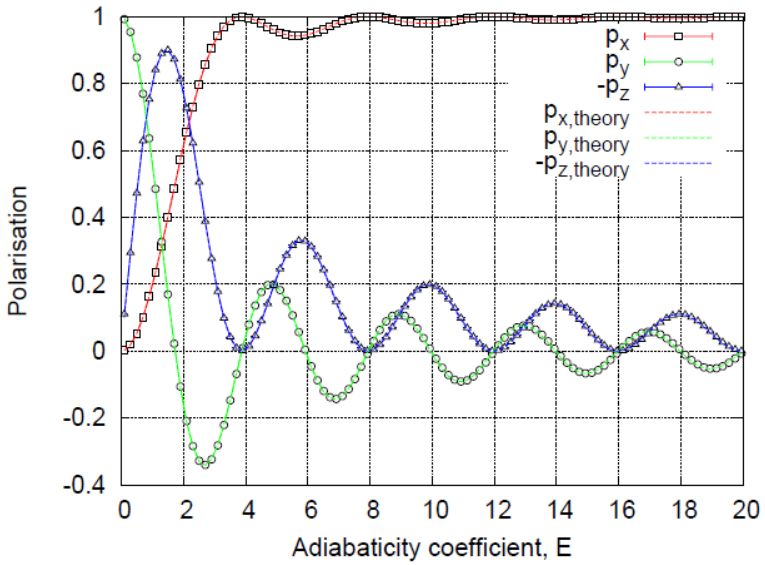

Adiabacity coefficient $E = -2\gamma B \Delta t/\pi$, where $\Delta t = m_n \lambda L/h$

See Knudsen et al., Submitted to Journal of Neutron Research (2012)

The SE-SANS Technique sketched

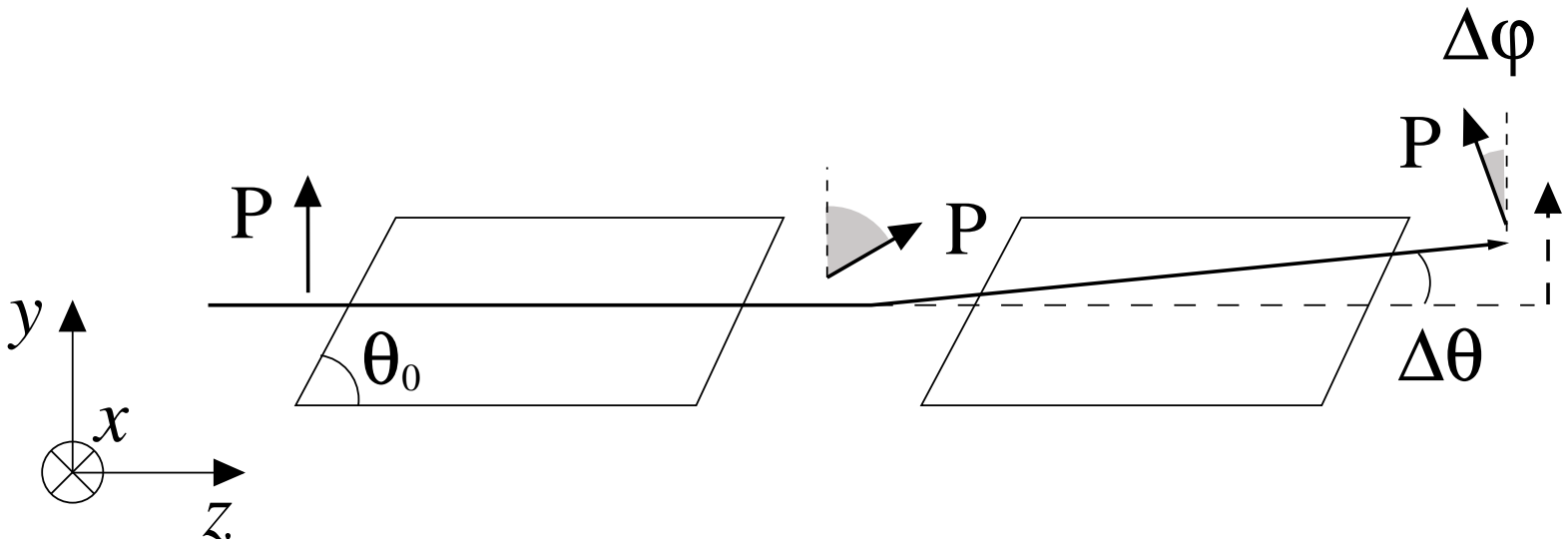

- The faces of the magnetic precession field **B** inclined by θ_0
- **B** aligned parallel and anti-parallel to the x-axis
- The trajectory of a neutron beam with polarisation vector **P** is deviated by $\Delta\theta$
  resulting in net difference in precession angle, $\Delta\varphi$

SE-SANS measures the transmission of polarisation $P(Z)$ which is directly related to the projection of the autocorrelation function of the sample density distribution along the neutron path.

Spin echo length ("the lengthscale at which sample features are probed"):

$$Z = \frac{c\lambda^2 L < \cot(\theta_0) >_\alpha}{2\pi} B$$

I.e. Z can be scanned by scanning B, λ or L.

In a virtual experiment anything can be scanned.

SE-SANS measures the transmission of polarisation $P(Z)$ which is directly related to the projection of the autocorrelation function of the sample density distribution along the neutron path.

Spin echo length ("the lengthscale at which sample features are probed"):

$$Z = \frac{c\lambda^2 L < \cot(\theta_0) >_\alpha}{2\pi} B$$

I.e. Z can be scanned by scanning B, λ or L.

In a virtual experiment anything can be scanned.

Why SE-SANS instead of traditional SANS?

- The divergence of the neutron beam is encoded, no need for hard collimation like classical SANS
- Good resolution of sizes (10^{-5}rad), competing with USANS
- Broad size-range: The special foil-flipper setup makes it possible to measure structures of sizes 5 nm-20 m size.

Rekveldt et al, Rev. Sci. Instr. **76** (2005)

Foil-flipper version of SE-SANS modelled

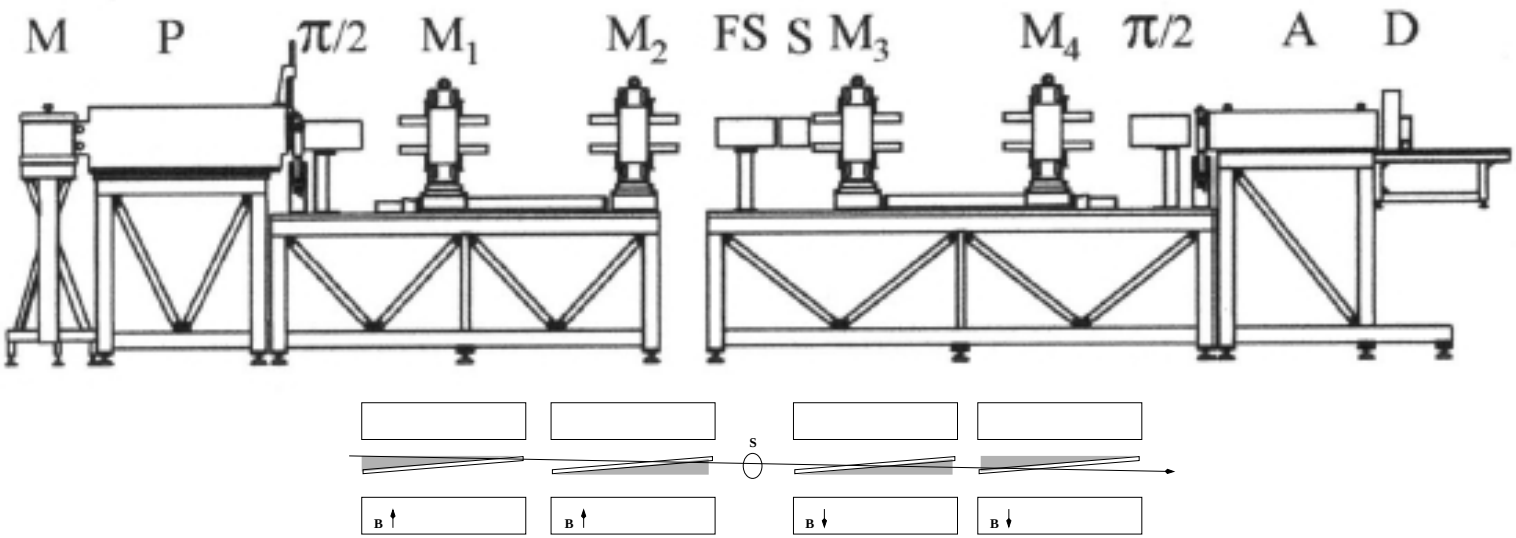

- The faces of the magnetized foils are inclined by θ_0
- **B** aligned parallel (and anti-parallel in the other set) to the y-axis
- The trajectory of a neutron beam with polarisation vector **P** is deviated by $\Delta\theta$
  resulting in net difference in precession angle, $\Delta\varphi$

Foil Flipper Magnets

Model is parameterized by:

- Pole shoe geometry.
- Spin-flip foil inclination.
- Magnetic field (correction) function inside.

Ideal: spin-flip in xz-plane.

The error may be corrected by a small $Bz \neq 0$ component.

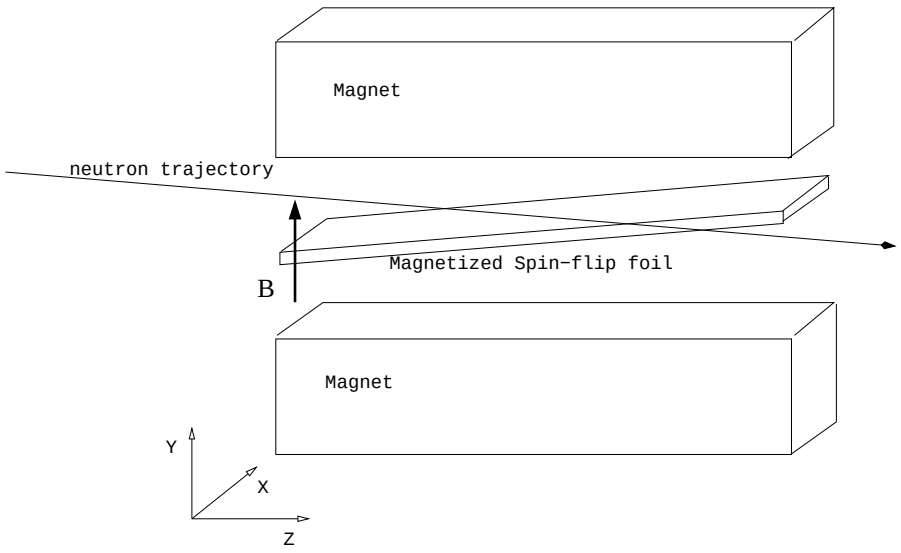

Foil Flipper Magnets

Model is parameterized by:

- Pole shoe geometry.
- Spin-flip foil inclination.
- Magnetic field (correction) function inside.

Ideal: spin-flip in xz-plane.

The error may be corrected by a small $Bz \neq 0$ component.

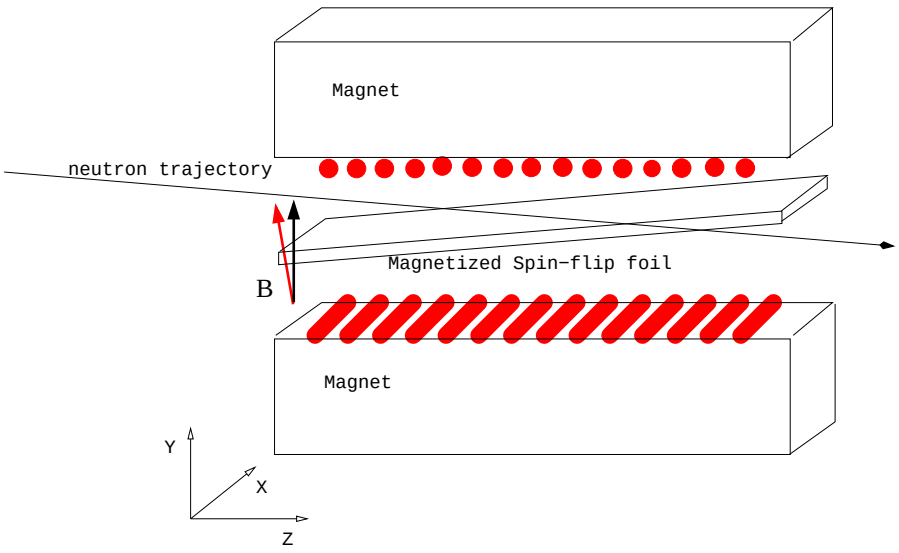

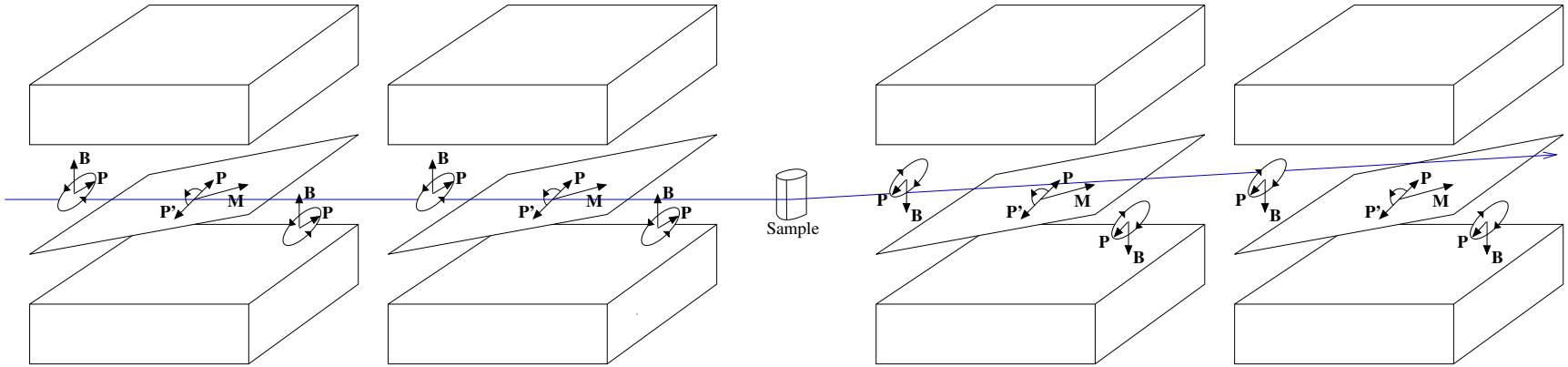

4 magnets → 2 sets of "regular" oblique SE-SANS precession sections → factor of 2 in spin echo length:

$$Z = \frac{c\lambda^2 L < \cot(\theta_0) >_\alpha}{\pi} B$$

Rekveldt et al Rev. Sci. Instr. **76**, 033901 (2005)

Idealized versions.

- Polariser (assuming unpolarised beam):

$$I_{in} = I_0,\ \mathbf{P}_{in} = (0,0,0) \quad \Rightarrow \quad I_{out} = \frac{I_{in}}{2}, \mathbf{P}_{out} = (0,1,0)$$

- Analyser:

$$I_{in} = I_0,\ \mathbf{P}_{in} = \mathbf{P} \quad \Rightarrow \quad I_{out} = I_0 \frac{1 + \mathbf{P} \cdot (0,1,0)}{2}, \mathbf{P}_{out} = (0,1,0)$$

...for polariser/analyser set to transmit $\mathbf{P} = (0,1,0)$

Sample - Aluminium wedge

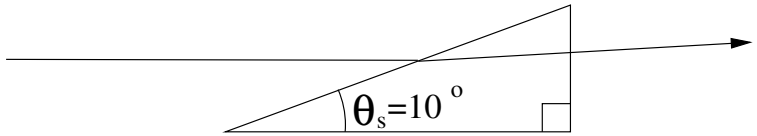

The refraction angle depends on the inclination angle of the wedge with respect to the average neutron beam direction as:

$$\Delta\theta = \frac{1}{2}\theta_c^2 \cot\theta_s \tag{1}$$

$\lambda = 0.2\,\mathrm{nm}$

$\theta_c = 1.85 \cdot 10^{-3}\,\mathrm{rad}$

$\Delta\theta = 9.75 \cdot 10^{-6}\,\mathrm{rad} = 0.00056^\circ$.

Sample model

- Aluminium wedge modelled as a forced scatterer
- Rotates all neutrons around the x-axis according to the specified scattering angle.
- No approximation of scattering angle for neutrons distributed around average beam direction along x
- but approximation for distribution of neutrons along y.

Sample model

- Aluminium wedge modelled as a forced scatterer
- Rotates all neutrons around the x-axis according to the specified scattering angle.
- No approximation of scattering angle for neutrons distributed around average beam direction along x
- but approximation for distribution of neutrons along y.

Sample model

- Aluminium wedge modelled as a forced scatterer
- Rotates all neutrons around the x-axis according to the specified scattering angle.
- No approximation of scattering angle for neutrons distributed around average beam direction along x
- but approximation for distribution of neutrons along y.

Sample model

- Aluminium wedge modelled as a forced scatterer
- Rotates all neutrons around the x-axis according to the specified scattering angle.
- No approximation of scattering angle for neutrons distributed around average beam direction along x
- but approximation for distribution of neutrons along y.

Phase shift

- The phase shift $\Delta\phi$ is found experimentally by tuning an external field outside the main precession regions.
- The polarisation is measured as a weighted difference of spin-up, I_u, and spin-down, I_d intensities.
- Small depolarisation without correction coil (• sample, ◦ empty)
- No depolarisation with correction coil (• sample, ◦ empty)

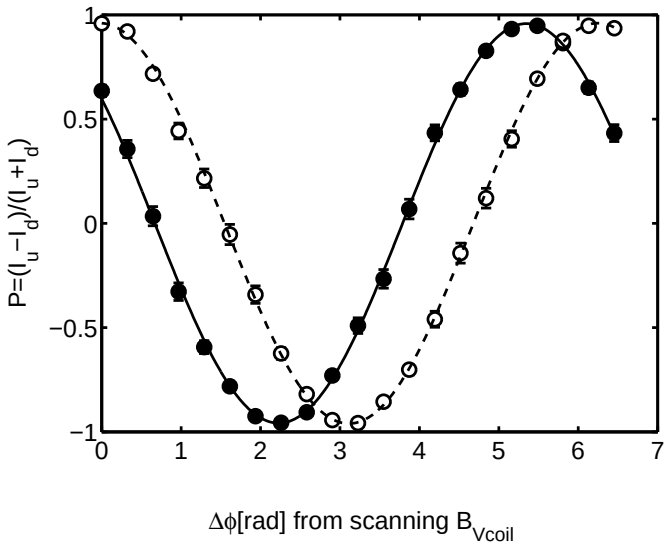

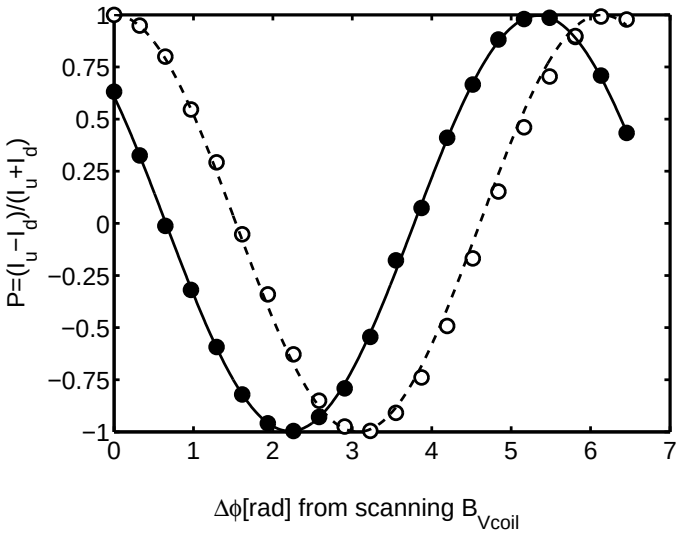

Phase shift

- The phase shift $\Delta\phi$ is found experimentally by tuning an external field outside the main precession regions.
- The polarisation is measured as a weighted difference of spin-up, I_u, and spin-down, I_d intensities.
- Small depolarisation without correction coil (• sample, ◦ empty)
- No depolarisation with correction coil (• sample, ◦ empty)

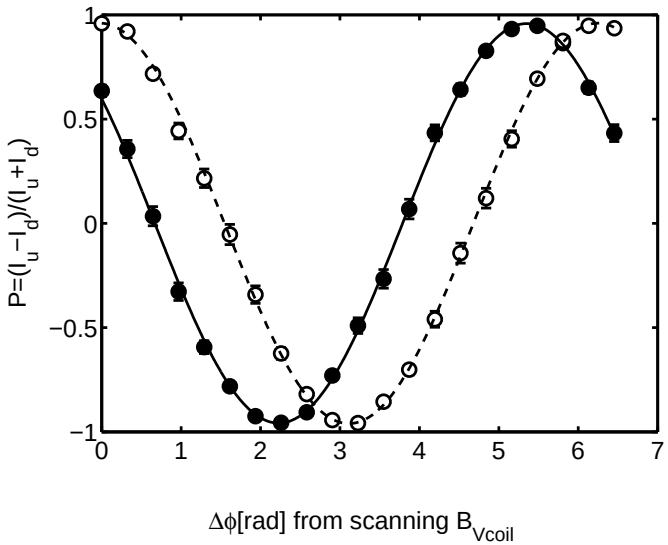

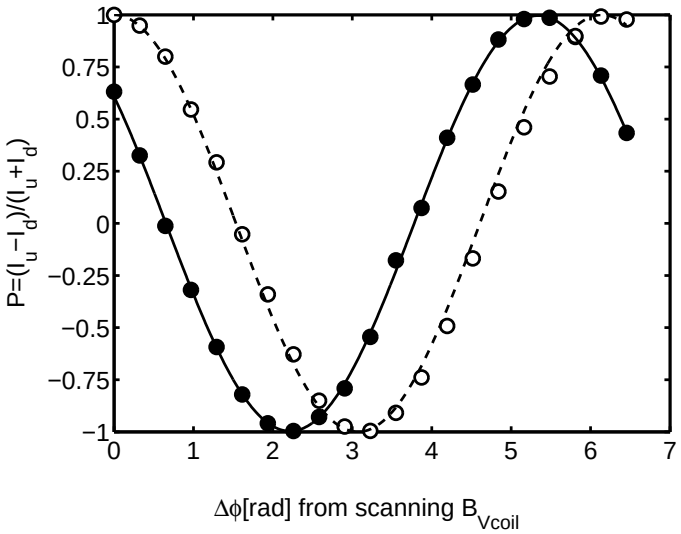

Phase shift

- The phase shift $\Delta\phi$ is found experimentally by tuning an external field outside the main precession regions.
- The polarisation is measured as a weighted difference of spin-up, I_u, and spin-down, I_d intensities.
- Small depolarisation without correction coil (• sample, ○ empty)
- No depolarisation with correction coil (• sample, ○ empty)

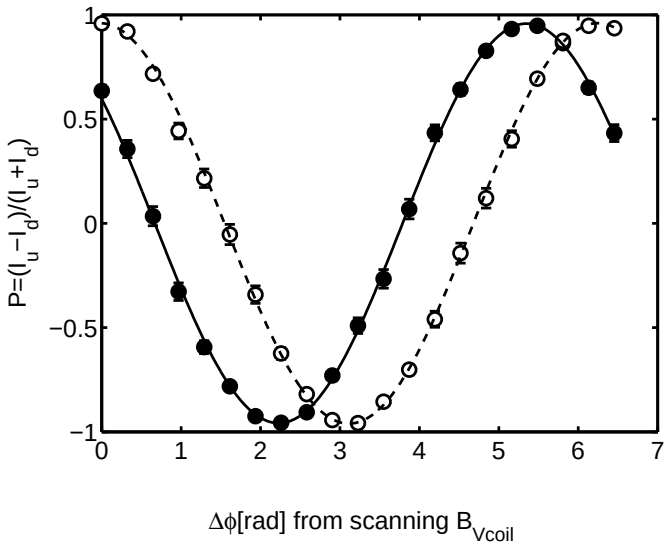

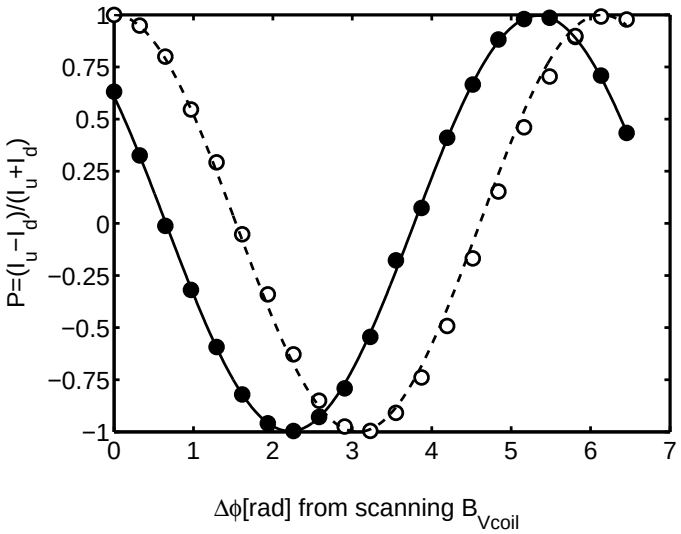

Phase shift

- The phase shift $\Delta\phi$ is found experimentally by tuning an external field outside the main precession regions.
- The polarisation is measured as a weighted difference of spin-up, I_u, and spin-down, I_d intensities.
- Small depolarisation without correction coil (• sample, ○ empty)
- No depolarisation with correction coil (• sample, ○ empty)

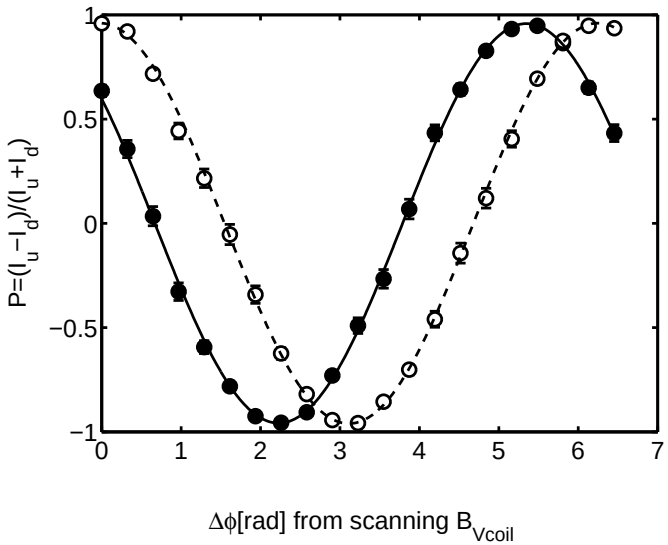

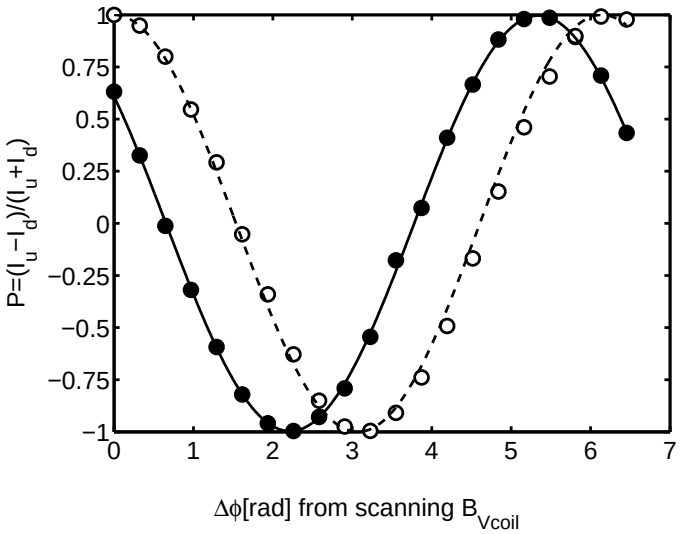

- There is a linear relation between phase shift and spin-echo length

$$\Delta\phi = N_b \frac{\lambda}{\tan\theta_s} \cdot Z \tag{2}$$

- N_b is the coherent scattering amplitude density of the refracting sample wedge material which we want to measure
- The spin-echo length was changed by changing the precession field B.
- For each new Z, the tuning field is scanned and the curve fit to a cosine to find the phase shift.

- Putting the right angle in the beam ($\theta_s = 45°$) gives scattering angle $2\Delta\theta$
- Eliminates the effects of slight misplacing of the θ_s angle.
- Simulated fitted slope of 0.11 rad/m compares well with measured fitted slope of 0.102(5) rad/m.

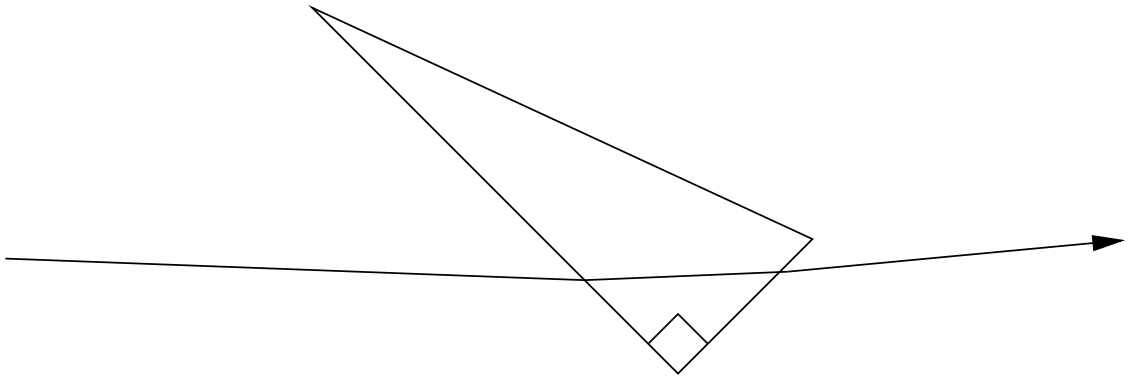

- Putting the right angle in the beam ($\theta_s = 45°$) gives scattering angle $2\Delta\theta$
- Eliminates the effects of slight misplacing of the θ_s angle.
- Simulated fitted slope of 0.11 rad/m compares well with measured fitted slope of 0.102(5) rad/m.

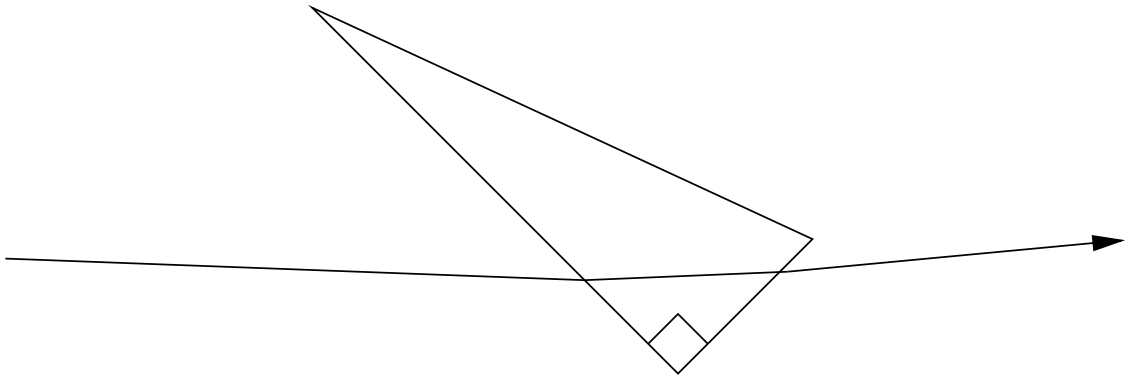

- Putting the right angle in the beam ($\theta_s = 45°$) gives scattering angle $2\Delta\theta$
- Eliminates the effects of slight misplacing of the θ_s angle.
- Simulated fitted slope of 0.11 rad/m compares well with measured fitted slope of 0.102(5) rad/m.

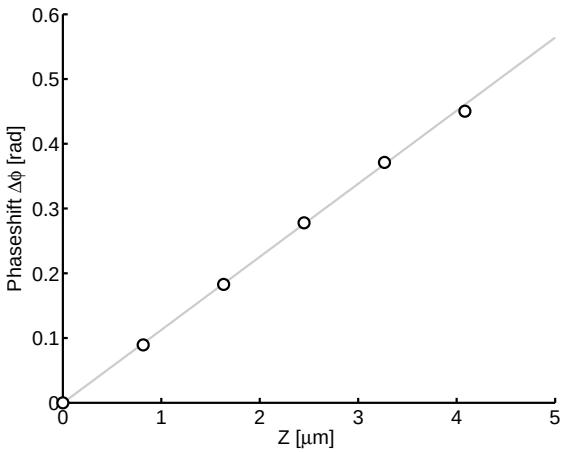

E. Knudsen, L. Udby et al, Physica B406 (2011)

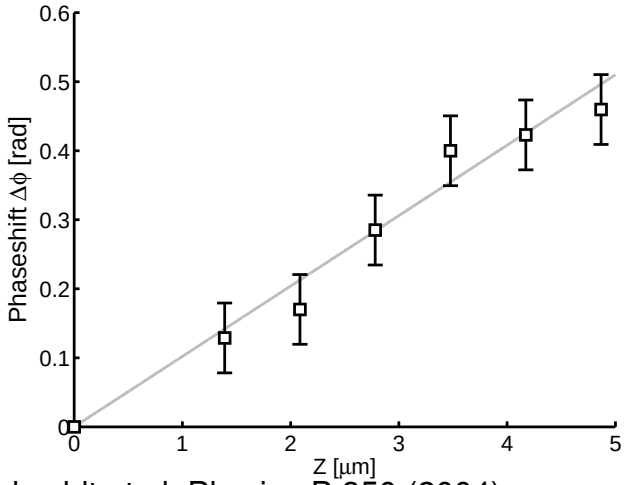

Rekveldt et al, Physica B 350 (2004)

- Putting the right angle in the beam ($\theta_s = 45°$) gives scattering angle $2\Delta\theta$
- Eliminates the effects of slight misplacing of the θ_s angle.
- Simulated fitted slope of 0.11 rad/m compares well with measured fitted slope of 0.102(5) rad/m.

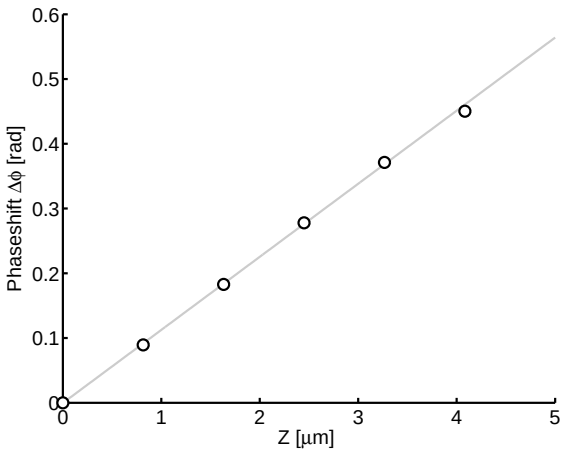

E. Knudsen, L. Udby et al, Physica B406 (2011)

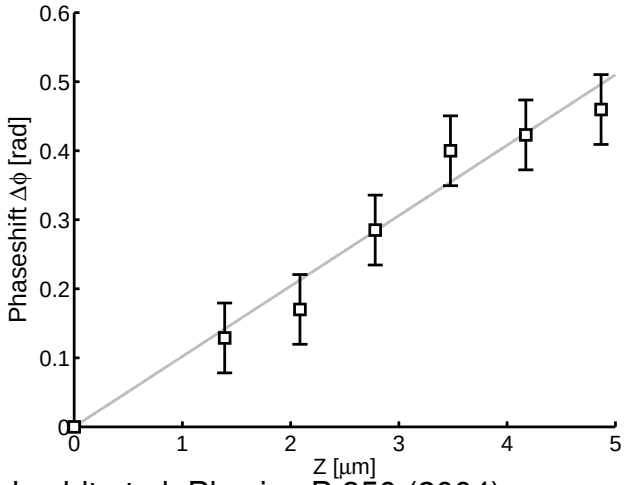

Rekveldt et al, Physica B 350 (2004)

We are on the way towards Virtual SE-SANS Experiments but much needs to be done

- Realistic magnetic fields
  stray fields, imperfections, read from Fin. Elem. Meth.
- Realistic polariser/analyser and $\pi/2$ rotator
- Other samples
- Implement source + guide + monochromator + detector efficiency models
- Further investigation of depolarisation effects

Want to know more? Take at look at Knudsen, Udby et al. Physica B **206** (2011)

We are on the way towards Virtual SE-SANS Experiments but much needs to be done

- Realistic magnetic fields
  stray fields, imperfections, read from Fin. Elem. Meth.
- Realistic polariser/analyser and $\pi/2$ rotator
- Other samples
- Implement source + guide + monochromator + detector efficiency models
- Further investigation of depolarisation effects

Want to know more? Take at look at Knudsen, Udby et al. Physica B **206** (2011)

We are on the way towards Virtual SE-SANS Experiments but much needs to be done

- Realistic magnetic fields
  stray fields, imperfections, read from Fin. Elem. Meth.
- Realistic polariser/analyser and $\pi/2$ rotator
- Other samples
- Implement source + guide + monochromator + detector efficiency models
- Further investigation of depolarisation effects

Want to know more? Take at look at Knudsen, Udby et al. Physica B **206** (2011)

We are on the way towards Virtual SE-SANS Experiments but much needs to be done

- Realistic magnetic fields
  stray fields, imperfections, read from Fin. Elem. Meth.
- Realistic polariser/analyser and $\pi/2$ rotator
- Other samples
- Implement source + guide + monochromator + detector efficiency models
- Further investigation of depolarisation effects

Want to know more? Take at look at Knudsen, Udby et al. Physica B **206** (2011)

We are on the way towards Virtual SE-SANS Experiments but much needs to be done

- Realistic magnetic fields
  stray fields, imperfections, read from Fin. Elem. Meth.
- Realistic polariser/analyser and $\pi/2$ rotator
- Other samples
- Implement source + guide + monochromator + detector efficiency models
- Further investigation of depolarisation effects

Want to know more? Take at look at Knudsen, Udby et al. Physica B **206** (2011)

We are on the way towards Virtual SE-SANS Experiments but much needs to be done

- Realistic magnetic fields
  stray fields, imperfections, read from Fin. Elem. Meth.
- Realistic polariser/analyser and $\pi/2$ rotator
- Other samples
- Implement source + guide + monochromator + detector efficiency models
- Further investigation of depolarisation effects

Want to know more? Take at look at Knudsen, Udby et al. Physica B **206** (2011)

We are on the way towards Virtual SE-SANS Experiments but much needs to be done

- Realistic magnetic fields
  stray fields, imperfections, read from Fin. Elem. Meth.
- Realistic polariser/analyser and $\pi/2$ rotator
- Other samples
- Implement source + guide + monochromator + detector efficiency models
- Further investigation of depolarisation effects

Want to know more? Take at look at Knudsen, Udby et al. Physica B **206** (2011)

I would like to thank my coworkers:

- McStas VE: Peter K. Willendrup (Risø DTU), Erik Knudsen(Risø DTU)
- Real Experiments: Wim Bouwmann (Delft),Jeroen Plomp (Delft)

Thank you for staying awake!